2016 年　第 35 卷　第 4 期　Vol.35　No.4

中 国 生 理 学 会

编者按：2011 年，中国生理学会成立 85 周年之际，学会编辑出版了以王晓民理事长为主编的上下两本图书，上册为《根深叶茂 蔚然成荫——中国生理学人物记》，下册为《根深叶茂 蔚然成荫——中国生理学团队记》。从 2013 年第 3 期开始，《生理通讯》将陆续转载，以飨读者。

生理学家

徐丰彦先生传略

张镜如

徐丰彦
（1903 年-1993 年）

徐丰彦，浙江淳安人，生于 1903 年 12 月 5 日，知识分子家庭出身。研究领域为植物性神经系统的调节功能，重点是心血管功能的神经调节。不幸于 1993 年 1 月 22 日病逝。

徐丰彦从小跟随祖父，在祖父执教的私塾求学。小学没有毕业，考上了父亲执教的中学。在中学时，功课很好，在班上考第一名，当过班长。中学毕业后，与几个同学一起来上海考大学；但由于山区教育的英语水平不高，未能考入大学。为了提高英语水平，插班进入复旦大学附中学习。通过努力，他的英语水平很快得到提高。

1923 年，他考入复旦大学理科。当时复旦大学理科并不强，进大学第二年郭任远教授又聘请了蔡翘、蔡堡、李汝祺等教授来加强理科师资队伍，他就转到心理学系学习。蔡翘老师是个实干家，工作非常努力，教他生理学、神经解剖学等课程。由于受蔡翘老师的影响很深，使他一辈子走上了生理学工作的道路。

1927 年大学毕业后，他随蔡翘老师到上海医学院任生理学助教。虽然条件不好，仍坚持跟蔡老师做科研。1930 年经蔡老师介绍，他到北京协和医学院进修，在林可胜教授指导下开始从事循环生理学科研。在林教授身边学习时间只有半年，但受益匪浅，而且决定了他长期从事循环生理研究的方向。

1932 年“一·二八”事变发生后，徐丰彦随蔡堡老师到中央大学任教，晋升为讲师。1933 年，他得到中华教育文化基金资助，经蔡翘老师介绍，赴英国伦敦大学 L. Evans 教授实验室进修。由于他手术精细、成功率高，深受 Evans 教授器重。在伦敦大学学习两年，完成了博士论文，顺利地通过了答辩。随后，他转到比利时，跟随 Heymans 教授进行颈动脉窦区的生理功能研究，时间只有半年，但决定了他从事颈动脉窦反射研究的方向。

1936 年徐丰彦从国外回来，经蔡翘老师介绍到中央研究院心理研究所工作，任副研究员，继续心血管反射的研究，完成了关于弥散性心血管张力反射的工作。这个工作是他与林可胜教授合作研究工作的延伸。1937 年，抗日战争爆发，他随心理研究所内迁，中间在长沙、衡山、阳朔停留过，后来被借调到贵阳医学院工作。1939 年下半年，蔡翘老师邀他去成都再次合作。当时，他在物资匮乏、空袭骚扰的条件下，坚持进行教学和研究，完成了较多的研究论文。在成都五年，是他研究工作最活跃的阶段，研究工作进展比较快。

1945 年初，徐丰彦受聘到重庆上海医学院，任生理学教授。不久抗战结束，1946 年

回到上海。当时上海医学院生理学科基本上是空白的，他抓起了重建生理学科室的工作，从招聘人员到设备建设，逐步把科室建立起来。1949 年后，他认识到国家急需大批建设人才，就专心致志地从事医学教育工作。此后 40 余年，他一直在上海医学院工作，培养了大量本科生、师资班学生、进修生和研究生，他的学生不少人已成为各地医学院校的学科带头人。

徐丰彦在助教阶段，在蔡翘指导下进行甲状旁腺与钙、磷代谢的研究，几年期间在《中国生理学杂志》上就发表了多篇研究论文。他在协和医学院进修期间，跟随林可胜进行了颈动脉窦压力感受性反射的研究，画出了窦内压和体循环动脉压之间的关系曲线，并指出在该曲线的中点（即正常血压水平时），压力感受性反射最敏感。这一论文于 1931 年发表。

他在英国进修两年期间，完成了博士论文工作，研究的内容是心肌乳酸代谢。由于心肌乳酸代谢研究不是他所渴望的工作，所以他转到 Heymans 教授实验室去进一步学习颈动脉窦区的生理功能研究。在回国后，他继续心血管反射的研究，并发现血管压力感受器并非仅仅存在于主动脉弓和颈动脉窦，而是广泛地存在于许多器官的血管中。因此，他提出了“弥散性血管张力反射”概念，在血压升高时广泛分布的压力感受器都能发生血管舒张反射，阐明了血管张力反射对循环的自我调节具有普遍性。与此同时，Heymans 也发表了相同的观点。

他在成都工作期间，完成了较多的科研论文。在这段时间内研究的重点是关于小肠平滑肌的兴奋性和神经支配特征。他研究了小肠平滑肌的化学兴奋性，测定了小肠乙酰胆碱和胆碱酯酶的含量，分析了肠－肠抑制反射的反射弧，发现了迷走神经对小肠运动的抑制作用。他提出假设，认为迷走神经中有胆碱能和肾上腺素能两种节后纤维。他对这一假设未获得机会亲自验证。

从 20 世纪 50 年代末开始，徐丰彦积极响应用现代科学方法整理和发扬祖国医学的号召，领导教研室人员从事气功疗法和针刺疗法生理机制的研究。在气功研究方面，基于现场观察和实验研究，他和教研室的同事共同提出了气功疗法生理机制的假设，认为人在练气功时通过意识控制呼吸，从而可间接地改变植物性神经系统的功能活动，达到治疗疾病的效果。这一成果获得了卫生部的奖励。在研究针刺的机制中，他亲自带领教研室的同志到医院观察“针刺麻醉”手术，并亲自体验针刺感觉。然后组织人员对针刺镇痛从临床实验到人体和动物实验进行研究。他提出了针刺有调整机体功能的作用，并着重研究针刺对调整异常心血管活动的机制的研究。通过多年来大量的实验研究，初步阐明了针刺和刺激躯体神经对实验性高血压、低血压、心律失常、血容量改变以及防御反应的调整作用的生理机制，在专业杂志上发表了一系列研究论文。这些成果曾多次获得部级科技成果奖。

徐丰彦在生理学教学方面也做了大量工作，成绩是卓著的。在担任生理学助教阶段，他为了配合蔡翘老师开展教学，认真带好实验，做好示教，自己动手做实验仪器，吹玻璃划刻度，亲自到野外去抓实验动物。在抗战内迁阶段，他在生活动荡的情况下，参考 Winton 和 Bayliss 的教科书编译了一本人体生理学书稿。这本书到 1952 年才出版发行，成为教师和学生的一本喜爱的生理学参考书。

1955 年前医学教育蓬勃发展，他集中精力搞好教学，为各种教学任务编写生理学讲义。1958 年卫生部组织的全国统编生理学教材内部出版发行，由他担任主编。该教材在试用二年后进行修订，于 1960 年正式公开发行，在全国起到了良好的作用。随后，1963 年第二版修订本再度发行，供全国医学院校采用。这本书在 1975 年打算再度修订出版，但由于当时考虑到内容分量过重，决定改编成生理学参考书。1978 年，这本参考书公开发行，称为《人体生理学》。1985 年起，在人民卫生出版社的指导下，组织了包括科研机构在内的 12 个单

位，邀请了 43 位 1989 年出版了第二版《人体生理学》。全书共分 10 篇、57 章，270 万字左右，是我国第一本生理学大型参考书。

徐丰彦出生在山区农村知识分子家庭，生活清苦，当地宗族势力很严重，家庭经常受人欺侮。他祖父为了不与当地人发生矛盾就去远地教书，怕人家找麻烦，一贯谨小慎微，做事规规矩矩。他随祖父生活十余年，祖父对他管教很严，养成了他严肃、慎微、孤僻的性格，平时不喜欢多讲话。

在他小学读书阶段，就已受到一定的爱国主义教育，懂得国家受人欺侮，我们自己应该把国家建设得富强起来。所以，他的爱国思想和正义感形成得比较早。在爱国主义思想的指引下。他一贯热爱祖国、追求真理，把自己的全部精力用在国家的教育和科学事业上。1956 年，他光荣地加入了中国共产党。他经常考虑的是如何发展和提高我国生理学的教学和科研事业，从不计较个人的名利和得失。在他的指导下，许多青年教师进行了科研工作，并由他帮助修改完成了论文，但他都不署自己的名字。1980 年，他主动让贤，辞去了教研室主任的职务，推荐年轻的同志接替。他还谢绝了领导上要他担任医学院院长的建议。他认为年轻人接替年长者的领导岗位是客观规律，也是科学教育事业兴旺发达的必由之路。

作为一名教育工作者，徐丰彦真正做到了严格要求，为人师表。他十分注意培养青年的独立工作能力和创造力，十分强调严肃谨慎、一丝不苟的科学作风。他为青年修改文稿时，连错别字也从不放过。他对人才培养一贯坚持德才并重，而更强调思想品德的重要性。他非常注意教师梯队的建设，注意选拔和培养带头人才。他认为带头人才不仅是业务尖子，更重要的是能顾全大局、善于团结人、与人合作共事、能带动一个集体共同前进。

作为一名科学工作者，他一贯孜孜不倦，不断探索，并且坚持真理，从不迷信盲从，人云亦云。当看到同事甚至领导在某个问题上是错误的，他总是直言不讳地指出，并以负责的态度说出自己的观点。他最痛恶那种明知上级的指示不正确，仍违心地说假话以迎合上级的做法。因此，他曾经受到不公正的待遇，曾被诬为“资产阶级学术权威”而遭批判。然而，他虽身处逆境，却仍处之泰然，坚持自己正确的观点，毫不动摇，表现了一个科学家尊重事实、坚持真理的可贵品格和勇敢精神。正因为如此，他受到同志们格外的尊敬。

生理学团队

北京大学生物膜与膜生物工程国家重点实验室

北京大学生物膜与膜生物工程国家重点实验室主要从事与离子通道及受体的信号转导机制、生物膜转运和动态变化过程、生物膜能量转换、膜蛋白结构与功能相关的神经生物学、心脏生理学、分子与细胞生理学方面的研究。

生物膜与膜生物工程国家重点实验室是依托于中国科学院动物研究所、清华大学和北京大学的联合研究基地，自 1986 年 9 月在三方单位领导的共同倡议下开始筹建，于 1988 年宣布成立，1990 年通过国家验收后正式向国内外开放，在 2011 年国家重点实验室评估工作中被评为“优秀”。实验室实行三方单位主任负责制，实验室主任负责各重大事项的决策与管理。围绕着生物膜这一关键科学领域，经过几届领导班子的全力建设，实验室正迅速成长为一支强大的科研和教学队

伍，形成了以中青年学者为主体，学术氛围浓厚、学术思想活跃、以学术交叉融合为特色、富有创新与钻研精神的科研队伍。生物膜与膜生物工程国家重点实验室北京大学分室的现任主任为王世强教授，分室现有固定人员及管理人员共 38 名，其中正高级职称 12 人、副高级职称 7 人；53%拥有博士学位；50 岁以下的成员占 84%。团队学术带头人共 12 人，其中教授 9 人、研究员 2 人、副教授 1 人。教育部“长江学者”计划特聘教授 3 人、科技部 973 项目首席科学家 3 人、“百千万”人才工程 1 人。面向国家重大需求和科学前沿，实验室积极承担国家级重大科研课题，五年来共承担了四十余项国家级科研任务、近十项国际合作交流项目，总经费愈六千万元。其中，国家“杰出青年基金”获得者 5 人、“973”项目 14 项、863 计划 2 项、基金委创新研究群体 1 个。

溯其渊源，北京大学生物膜与膜生物工程国家重点实验室是在原北京大学生物学系生理学、生物物理学两个教研室基础上组建的。1952 年全国院系调整后，著名生理学家、中国生理学会前理事长赵以炳先生在北大组建了生理学教研室，开设了我国第一个生理学专业。在 20 世纪五六十年代与苏联合作时期，建立了条件完备的巴甫洛夫条件反射实验室，成为我国神经生理学研究的核心基地之一，周恩来总理曾自豪地带领外国领导人访问该实验室。70 年代末，实验室的研究方向根据当时生理学前沿领域，重点建设了电生理学专业，并在心肌电生理、神经突触传递、冬眠神经调节与生理适应、神经与免疫系统相互作用、神经毒素作用机制、低等动物感觉与运动机能等多个方面开展了卓有成效的研究工作。到了 80 年代末，青年一代学术带头人在上述研究平台的基础上，组建了生物膜与膜生物工程国家重点实验室北大分室，成为我国当时在离子通道研究方面最先进的实验室之一。90 年代以来，随着国际生理学和神经科学的发展，在已有的优势基础上，拓展了神经递质与受体的分子生物学、细胞钙信号转导、细胞膜动态变化及其调控等前沿领域。21 世纪以来，实验室先后配备了蔡司 LSM-510Meta 型激光共聚焦/双光子扫描成像系统、多套膜片钳和其他配套的电生理设备，并且将膜片钳和激光共聚焦扫描成像系统优化组合起来，能达到同步触发并扫描记录的国际先进水平；此外，常规生化分子生物学仪器齐全，拥有装备精良的细胞培养室，以上这些成熟的研究条件为开展科研工作提供了关键技术支撑平台。随着在人才引进、梯队建设等诸多方面的明显提升，实验室在离子通道、囊泡分泌、核膜动态、膜蛋白结构与功能、神经递质受体等方面形成研究特色，并在跨膜钙信号转导的微观动态方面居国际领先水平。

实验室主要招生专业为生理学，涵盖了痛觉/成瘾的神经机制、细胞钙信号转导、脑疾病的神经生物学、心脏疾病的细胞分子机制、发育神经生物学、冬眠与低温低氧适应机制、基因与行为的神经生物学等多个研究方向。作为我国综合性大学中仅有的生理学专业之一，北京大学生理学专业以北大强大的数理化学科为依托，以生物多样性、动物与环境相互作用为背景，面向丰富多彩的人和动物机能，以阐明人和动物生理过程的基本规律为己任，具有鲜明的自然科学特色。自 50 年代以来，北京大学曾连续招收培养生理学专业本科学生。恢复学位制度以来，北京大学生理学专业先后成为教育部首批公布的硕士点、博士点、博士后流动站、国家级重点学科。所培养的近千名学生中，许多已成为中、美等国神经生物学和生理学领域成就卓著的科学家。

长期以来，实验室围绕生理学领域开展了大量基础研究，取得了一系列科研成果。例如在深入研究跨膜钙致钙释放的微观动态和分子调控中，首次发现并提出了“钙闪烁”的新概念，阐明了跨膜钙信号转导过程在细胞迁移中的重要作用。该工作在 Nature 等期刊发表，

开辟了一个新研究视野。近 5 年来，实验室共发表 SCI 论文百余篇，获授权发明专利两项（国内、国外各一项）。荣获各类奖励六项，其中王世强教授于 2007 年获“有突出影响的心血管论文奖”、陈建国教授于同年获上海市科学技术奖一等奖、程和平教授获 2008 年度“长江学者成就奖”。

自成立以来，实验室始终具有广阔的国际视野，非常注重与国内外学术界的学术交流和合作。近年来已成功承办过两次国际性会议、常邀请国外优秀学者前来讲学、派遣研究人员赴国外访问。此外，还设立实验室开放基金吸引国内外优秀学者到实验室开展研究，并将实验室的研究工作与国内外的学术活动相结合，活跃了实验室的创新研究氛围，增强了实验室在生物膜领域的学术地位。目前已与香港科技大学、美国哈佛大学、斯坦福大学、Burnham Medical Research Institute 等多家国际学术机构建立了长期稳定的合作关系，在各自的优势领域取长补短，建立了广泛而扎实的国内、国际联系网络。

张锡钧基金

编者按：2015 年 10 月 24 日-25 日中国生理学会张锡钧基金会第十三届全国青年优秀生理学学术论文交流会在湖北武汉顺利召开。由各省生理学会推荐的 47 名参赛选手的论文参加评选，会议展示了选手们近 3 年来在生理学研究方面所取得的最新研究成果。经过专家对参评者论文和现场报告的综合评判，评出一等奖 1 名、二等奖 2 名、三等奖 3 名；最佳表达奖、最佳答辩奖、最佳图表奖各 1 名。从 2015 年第 5 期开始，《生理通讯》将陆续转载获奖者的参评论文各一篇，以飨读者。

Superficial Layer-Specific Histaminergic Modulation of Medial Entorhinal Cortex Required for Spatial Learning

Chao He[1,†], Fenlan Luo[1,†], Xingshu Chen[2], Fang Chen[1], Chao Li[1], Shuancheng Ren[1], Qicheng Qiao[1], Jun Zhang[1], Luis de Lecea[4], Dong Gao[3],and Zhian Hu[1]

[1]Department of Physiology, [2]Department of Histology and Embryology, [3]Department of Sleep and Psychology, Institute of Surgery Research, Daping Hospital, Third Military Medical University, Chongqing 400042, PR China, and [4]Department of Psychiatry and Behavioral Sciences, Stanford University, Palo Alto, CA 94304, USA

Address correspondence to Prof. Zhian Hu. Email: zhianhu@aliyun.com

†C.H. and F.L. contributed equally to this work.

The medial entorhinal cortex (MEC) plays a crucial role in spatial learning and memory. Whereas the MEC receives a dense histaminergic innervation from the tuberomamillary nucleus of the hypothalamus, the functions of histamine in this brain region remain unclear. Here, we show that histamine acts via H_1Rs to directly depolarize the principal neurons in the superficial, but not deep, layers of the MEC when recording at somata. Moreover, histamine decreases the spontaneous GABA, but not glutamate, release onto principal neurons in the superficial layers by acting at presynaptic H_3Rs without effect on synaptic release in the deep layers. Histamine-induced depolarization is mediated via inhibition of Kir channels and requires the activation

of protein kinase C, whereas the inhibition of spontaneous GABA release by histamine depends on voltage-gated Ca^{2+} channels and extracellular Ca^{2+}. Furthermore, microinjection of the H_1R or H_3R, but not H_2R, antagonist respectively into the superficial, but not deep, layers of MEC impairs rat spatial learning as assessed by water maze tasks but does not affect the motor function and exploratory activity in an open field. Together, our study indicates that histamine plays an essential role in spatial learning by selectively regulating neuronal excitability and synaptic transmission in the superficial layers of the MEC.

Key words: histaminergic system, kir channels, medial entorhinal cortex, spatial learning
Cerebral Cortex, April 2016;26: 1590–1608 | DOI: 10.1093/cercor/bhu322

Introduction

The entorhinal cortex (EC) is widely regarded as the hub of corticohippocampal circuits (Witter et al. 1989; Witter et al. 2000). It has been divided into 2 subregions, the medial EC (MEC) and the lateral EC (LEC) (Canto et al. 2008; Van Cauter et al. 2013). The MEC contains spatially tuned neurons and is closely related to the path integration and spatial learning (Fyhn et al. 2004; Sargolini et al. 2006; Solstad et al. 2008; Suh et al. 2011; Van Cauter et al. 2013; Zhang et al. 2013; Zhang et al. 2014). Multimodal sensory information from various cortical areas converges onto neurons inthe superficial layers (Layers II/III) of the EC, where it is processed and relayed into all subregions of the hippocampus (Burwell 2000; van Strien et al. 2009). In contrast, the deep layers of EC (Layers V/VI) receive the outputs from the CA1 and subiculum and then convey the highly processed sensory information to superficial layers of the EC (Dolorfo and Amaral 1998; van Haeften et al. 2003) and to other cortical areas (Witter et al. 1989; van Strien et al. 2009).

Consistent with the different anatomical connection patterns, the superficial and deep layers of the EC are functionally separated in the memory-encoding and replaying processes, respectively, and display different activity patterns across the distinct brain states (Chrobak and Buzsaki 1994; Buzsaki 1996; Battaglia et al. 2011). During the exploratory behavior, neurons in the superficial, but not deep, layers of the EC are highly active and their discharges are phase-locked to the negative peak of theta-coupled gamma oscillations (40–100 Hz) (Chrobak and Buzsaki 1994, 1998). The active state of the neurons in the superficial layers is required for the spatial information encoding as suppression of these neurons caused a dramatic impairment in rat learning phase (Chrobak et al. 2000; Deng et al. 2009; Igarashi et al. 2014). Interestingly, during awake immobility and slow-wave sleep, neurons in the superficial layers exhibit slow oscillation (<1 Hz) and become relatively silent compared with active wakefulness (Chrobak and Buzsaki 1994; Isomura et al. 2006; Hahn et al. 2012). At these off-line brain states, neuronal discharges in the deep, but not superficial, layers of the EC in conjunction with sharp-wave ripples are thought to be critical for the memory replaying and consolidation (Chrobak and Buzsaki 1994; Li et al. 2008; Ramadan et al. 2009; Inostroza and Born 2013).

Although it is evident that the neuronal activity in the superficial layers shows alternative potentiation and depression across distinct brain states, it is unknown which physiological modulators contribute to these effects. It is particularly interesting to consider that the arousal-promoting systems might to a large extent

control the activity patterns in superficial layers of the EC since their activity exhibits a strong circadian variation. The histaminergic system, originating exclusively from the tuberomamillary nucleus (TMN) of the hypothalamus but projecting extensively to almost all the brain regions, represents a prominent arousal-promoting system in the central nervous system (CNS) (Lin 2000; Anaclet et al. 2009; Lin, Anaclet, et al. 2011; Lin, Sergeeva, et al. 2011) and is implicated in the regulation of several arousal-related physiological processes including learning and memory (Haas and Panula 2003; Haas et al. 2008; Alvarez 2009). Anatomically, the EC receives an extensive innervation from the histaminergic neurons (Airaksinen and Panula 1988). In normal human brain, it has been reported that histamine-containing nerve fibers were densely distributed in the superficial, but not the deep, layers of the EC (Panula et al. 1998). Moreover, histaminergic neurons specifically discharge at high rates during wakefulness, especially during attentive waking (Vanni-Mercier et al. 2003; Takahashi et al. 2006) and are closely related to theta oscillation in the hippocampal formation (Hajos et al. 2008). This activity pattern of the histaminergic neurons is highly correlated with that of neurons in the superficial, but not deep, layers of the EC.

Currently, the functions of histamine in the EC are still elusive. In the present study, we tested the hypothesis that histaminergic system might selectively increase the activity of the principal projection neurons in the superficial layers of the EC and thus facilitate superficial layer-dependent memory-encoding processes. Nevertheless, histamine might not affect the neuronal activity in the deep layers as they function during the off-lines states, during which the levels of histamine are relative low. Using a combination of electrophysiology, behavioral pharmacology, and immunohistochemical approaches, our results reveal the superficial layer-specific effects of histamine in regulation of neuronal excitability, neurotransmission, and spatial learning. Thus, these findings provide a novel pathway that at least partially explains the role of histaminergic system in spatial cognition and the different activity levels of the superficial layers in the MEC across distinct brain states.

Materials and Methods

Brain Slice Preparation

All experimental procedures involving animals were in compliance with the guidelines for the care and use of laboratory animals in the Third Military Medical University. Acute brain slices were obtained from male Sprague–Dawley rats (P14–20) by methods that have been described in detail previously (Li et al. 2011). Semi-horizontal slices (400 μm) containing the EC were prepared with an oscillating tissue slicer (Leica, VT1000) in an ice-cold section solution equilibrated with 95% O_2 and 5% CO_2 containing (in mM): sucrose, 220; KCl, 2.5; NaH_2PO_4, 1.25; $NaHCO_3$, 26; $MgCl_2$, 6; $CaCl_2$, 1; and glucose, 10. The slices were initially incubated for at least 1 h at room temperature (20–24°C) in oxygenated (95% O_2–5%CO_2) artificial cerebrospinal fluid (ACSF, composition in mM: NaCl 124; KCl 3; $NaHCO_3$, 26; $MgCl_2$, 2; $CaCl_2$, 2; and glucose 10). During recording sessions, the slices were transferred to a submerged chamber and continuously superfused with oxygenated (95%O_2–5%CO_2) ACSF at room temperature.

Whole-Cell Clamp Recordings

Targeted neurons were verified with an upright

microscope equipped with Leica differential interference contrast optics and an infrared video imaging camera. Whole-cell recordings were performed on neurons with glass pipettes (3–5 MΩ) filled with an internal solution (composition in mM: potassium gluconate 125; KCl, 20; Hepes, 10; EGTA, 1; $MgCl_2$, 2; ATP, 4; adjusted to pH 7.2–7.4 with 1M KOH). For recordings of spontaneous miniature inhibitory postsynaptic currents (mIPSCs), at a holding potential of −60 mV, a Cs^+ pipette solution (composition in mM: CsCl, 145; Hepes, 10; $MgCl_2$, 2; EGTA, 1; ATP, 2; adjusted to pH 7.2–7.4 with 1 M CsOH) was used. Recording pipettes approached toward targeted neurons in the slice under positive pressure. After tight seal formation on the order of 1–2 GΩ made by negative pressure, the membrane patch was then ruptured by suction. Data were collected after at least 5 min of stabilization from the formation of whole-cell configuration unless stated otherwise. During recording sessions, series resistance was compensated 50–70% and cells were excluded from the study if the series resistance increased by >15% during recording or exceeded 20 MΩ. Unless stated otherwise, all the recordings were performed at room temperature.

Data were acquired with an EPC10 amplifier (HEKA Elektronik, Lambrecht/Pfalz) and stored for off-line analysis with Pulse/Pulsefit v.8.74 (HEKA Elektronik) and Igor Pro v.4.03 (WaveMatrics). The output signal was low-pass-filtered at 4 kHz and digitized at 10 kHz. To investigate the direct effect of histamine, histamine was puffed on the slice for 1 min. This drug application method has been described in detail in our previous study (Li et al. 2010). The mean membrane potential or holding current obtained during the last 6 s of the histamine application session was used for analysis and compared with baseline. For the miniature excitatory postsynaptic currents (mEPSCs) and mIPSCs, the methods for recording and analysis of these events were similar to those described elsewhere (Li et al. 2011). In brief, after stably recording of the baseline at least 2 min, histamine was bathed to the slices for 6 min. mEPSCs and mIPSCs recorded at last 2 min of the application session were analyzed, and their frequency and amplitude were compared with that of the baseline. Action potential, spontaneous mEPSCs, and mIPSCs were determined automatically by using Mini-analysis software (version 6.0, Synaptosoft). The detected synaptic events have fast onset and exponential decay kinetics, and obviously erroneous events were excluded manually by visual examination. The parameters for detecting synaptic events were identical in each cell in the absence or presence of drugs.

Cannula Implantation and Microinjection

Male Sprague–Dawley rats weighing 240–250g were used in the behavioral tests. All animals were housed individually in thermoregulated (22–24°C) Plexiglas cages with a 12 h of light/dark cycle (lights on at 7:00 A.M.). The rats had ad libitum access to food and water.

All surgical procedures were performed under aseptic conditions. The rats were anesthetized with intraperitoneal injection of 2.5% sodium pentobarbital (2 mL/kg) and placed on a stereotaxic frame. The cranial surface was exposed by removal of the scalp, and the bregma was identified and used as the stereotactic reference point. Two stainless-steel guide cannulae (length 11 mm, o.d. 0.64 mm, and i.d. 0.45 mm) for the microinjection cannulae were bilaterally implanted into the superficial or deep layers of the MEC of each animal. The guide cannulae were secured to

the skull with 2 stainless-steel skull screws and dental acrylic. The coordinates for the implantation were based on the rat brain atlas of Paxinos and Watson (2007) (superficial layers: AP −8.4 mm, ML ±4.4 mm, and DV −5.6 mm; deep layers: AP −8.3 mm, ML ±4.8 mm, and DV −4.6 mm). Each guide cannula was provided with a stainless-steel mandril to prevent obstruction. The drug microinjection approach is similar to that described in our previous study (Cun et al. 2014). In brief, at the time of infusion, an injection cannula (length 11.5 mm, o.d. 0.41 mm, and i.d. 0.25 mm) was inserted to protrude 0.5 mm beyond the tip of the guide cannula for microinjection of ACSF, H_1R antagonist triprolidine (2 μM), H_2R antagonist ranitidine (30 μM), and H_3R antagonist clobenpropit (8 μM) using Hamilton syringes (0.5 μL/side, lasting 2 min). After microinjection, the injection cannula was left for an additional 2 min before a withdrawal to reduce efflux of ACSF or drugs.

Morris Water Maze Test

Behavior tests were conducted after 5 days of postsurgical recovery. All rats were trained in a white Morris water maze (diameter, 120 cm; height, 50 cm; water depth, 40 cm; and water temperature, 23 ± 2°C). The water was made opaque by the addition of semi-skimmed milk, which prevents the animals from seeing the platform. The pool was located on an elevated platform 20 cm above the floor in the center of a brightly lit room containing salient visual cues such as geometric shapes, wall posters, and electrical fittings on the wall. The swimming paths were tracked by a computer-assisted video-tracking device system that allows measurement of a number of parameters, including latency to find the platform, swimming distance, swimming speed, and quadrant analyses.

All rats were trained to find a hidden platform (10 cm in diameter, submerged 1 cm) in a water maze using protocols mentioned previously (Deng et al. 2009). They received 2 days of training, each day comprising 6 consecutive trials. The platform remained constant across all the trials. During the trials, rats were gently placed in the water maze facing the wall with 4 start positions varied in a predetermined and pseudorandom order. Each trial lasted for 60 s or until the rat successfully located the platform, with a 30-s intertrial interval. The rat that failed to find the platform within 60 s was guided to the platform by the experimenter and allowed to stay on the platform for 30 s before next trial. Six hours after completion of acquisition trials, a probe trial with the platform unavailable for 90 s was carried out. The rats were placed at the pool side opposite to the target quadrant. Probe trial performance of each group was expressed by the proportion of total time spent in each quadrant of the Morris water maze. The random level spent in each quadrant of the Morris water maze is 25%. Rats received ACSF or drug infusion 15 min prior to the training on Days 1 and 2 but no drug treatment before probe trial.

Open-Field Test

A square open field (50 cm × 50 cm × 40 cm) lit with 2 60-W floodlights above the field was used to assess general activity of rats. The movement and behavior of the rats were recorded by a computer-assisted video-tracking system, which allows measurement of a number of parameters, including movement distance and number of rearings. Rats received ACSF or drug infusion 15 min prior to the open-field test. After placing a rat at the center of the arena, the movement distance and number of rearings, which represent

locomotor activity and exploratory activity, respectively, were recorded for 5 min.

Histological Identification

The method used to identify the injection sites in the present study was similar to that described in previous study (Deng et al. 2009). In brief, after completion of the behavioral tests, rats were anesthetized with an overdose of sodium pentobarbital and perfused transcardially with saline followed by 4% paraformaldehyde. The brains were removed and then stored in 30% sucrose and 4% paraformaldehyde solution for dehydration. Frozen sections were prepared (30 μm) from the dorsal to the ventral and stained with cresyl violet. By visualizing the sections with an inverted microscope, the track of cannulae from dorsal to ventral can be identified. The last section from dorsal to ventral containing the injection hole was selected, and this site was regarded as the drug injection site. The injection sites were confirmed in the present study. Data from the rats with incorrect injection sites were excluded from analysis.

Immunohistochemistry

Sprague–Dawley rats (weighing 200–250 g) were anesthetized deeply with 2.5% sodium pentobarbital (2.4–2.8 mL/kg, intraperitoneal) and then perfused transcardially with 300 mL normal saline, followed by 500 mL of 4% paraformaldehyde in 0.1 M phosphate buffer. Brains were removed, postfixed for 12 h at 4°C in 4% paraformaldehyde, and then cryoprotected with a 4% paraformaldehyde and 30% sucrose solution in phosphate buffer for 48 h. Horizontal sections (30 μm) containing the MEC were prepared by using a freezing microtome (CM 3050S, Leica). The sections were first incubated in 10% normal bovine serum for 30 min and then incubated overnight at 4°C with primary antibodies to H_1Rs or H_2Rs: a rabbit anti-H_1R polyclonal antibody (1:100; Santa Cruz Biotechnology) or a rabbit anti-H_2R polyclonal antibody (1:50; Santa Cruz Biotechnology). The specificity of anti- H_1R and anti-H_2R primary antibodies has been tested in other studies (Peng et al. 2013; Zhuang et al. 2013). After washing in PBS, these sections were incubated in the fluorescein-labeled secondary antibody solutions (goat anti-rabbit 1:2000; Invitrogen) for 2 h at room temperature in the dark and then mounted onto slides with coverslips. For double staining of immunofluorescence, the sections were washed with PBS 3 times, blocked with 1% BSA (bovine serum albumin) and 0.4% Triton X-100 for 30 min in 37°C. The sections were incubated with the first primary antibodies rabbit anti-H_3Rs (1:300, Sigma) overnight at 4°C. The specificity of anti-H_3R primary antibodies has been checked in the brain neurons according to the product information. After washing with PBS 3 times, the sections were incubated with Alexa 568-conjugated donkey anti-rabbit secondary antibody (1:500, Invitrogen) at 37°C for 2 h. Then, the sections were blocked again with 1% BSA and 0.4% Triton X-100 for 30 min in 37°C, incubated with the second primary antibodies goat anti-GAD-67 (1:200, Santa Cruz Biotechnology) overnight at 4°C. The sections were washed with PBS 3 times, incubated with Alexa 488-conjugated donkey anti-goat secondary antibody (1:500, Invitrogen) at 37°C for 2 h. The sections were washed with PBS 3 times, then nuclear-stained with 0.01% 4′, 6′-diamidino-2-phenylindole (DAB, Sigma), and mounted onto coverslips with Glycergel mounting medium (Dako). Negative controls had

PBS or polyclonal rabbit immunoglobulin G (Santa Cruz Biotechnology) instead of the primary antibody. All images were taken with an inverted laser scanning confocal microscope (FV1000; Olympus).

Drugs

Histamine, triprolidine, ranitidine, clobenpropit, 6-cyano-7-nitroquinoxaline-2,3-dione (CNQX), D-2-amino-5-phosphonovaleric acid (AP5), picrotoxin (PIC), tetrodotoxin (TTX), $BaCl_2$, CsCl, bisindolylmaleimide II (BIS-II), and tetraethylammonium (TEA) were purchased from Sigma. Voltage-dependent potassium channel blocker 4-aminopyridine (4AP) was obtained from Tocris Cookson. Histamine, triprolidine, ranitidine, clobenpropit, AP5, TTX, $BaCl_2$, CsCl, TEA, and 4AP were dissolved in ACSF, whereas CNQX, PIC, and BIS-II were dissolved in dimethyl sulfoxide. All drugs were prepared as concentrated stock solutions and frozen at -20°C until use. The drugs from stock were freshly diluted to the desired concentrations. The final concentration of dimethyl sulfoxide did not exceed 0.1%.

Data Analysis

Values were presented as the means ± SEM. Student's paired or unpaired *t*-test, Kolmogorov–Smirnov (K–S) test, one-way, and repeated-measures' analysis of variance (ANOVA), and Fisher's protected least significant difference (LSD) post hoc testing were used for statistical analysis. Significant differences were accepted at $P < 0.05$.

Results

Histamine Specifically Increases the Excitability of Principal Neurons in the Superficial, but not Deep, Layers of the MEC

Stellate neurons are the most prominent principal projection neurons in the superficial layers of the MEC. These neurons are primarily located in Layer II and the border between Layer II and Layer III and have a polygonal soma with multiple thick sparsely primary dendrites radiating out from the cell body (Supplementary Fig. 1A, B). A notable feature of stellate neurons is that they showed profound depolarizing voltage sags in response to hyperpolarizing current pulses (Fig. 1A and Supplementary Table 1) and had larger hyperpolarization-activated currents in voltage-clamp recordings (Supplementary Fig. 1C and Supplementary Table 1). This unique electrophysiological feature is attributed to stellate neurons expressing a high level of hyperpolarization-activated, cation nonselective channels at their somata (Nolan et al. 2007).

Considering the finding of moderately dense histaminergic innervation in the EC, we carried out current- or voltage-clamp recordings to examine the effect of histamine on the activity of stellate neurons in the superficial layers of the MEC. Under current-clamp mode, local application of histamine (1–1000 μM) significantly depolarized the membrane potential on a majority of the recorded stellate neurons (76.3%, 61/80). The depolarization was reversed following washout and sufficient to stimulate an increase in firing frequency in part of the recorded cells. The histamine-induced excitation on stellate neurons was concentration dependent. Local application of 1, 10, 100, and 1000 μM histamine generated a membrane depolarization of 1.1 ± 0.1 mV ($n = 4$), 3.3 ±0.3 mV ($n = 12$), 6.3 ± 0.5 mV ($n = 3$), and 6.5 ± 0.6mV ($n = 3$), respectively ($F_{3, 21} = 28.30$; $P < 0.001$; one-way ANOVA; Fig. 1B,C). We also recorded the holding currents of stellate neurons

in voltage-clamp at −60 mV, a potential close to the resting membrane potential. Under these conditions, application of histamine (10 μM) significantly induced an inward current (control: −25.1 ± 11.7 pA; histamine: −52.0 ± 13.9 pA; n=5; P < 0.01; paired t-test; Fig. 1D).

Accordingly, we also investigated the effect of histamine on the superficial pyramidal neuron activity, another type of principal projection neurons that were identified by their morphology, location, and electrophysiological properties (Supplementary Fig. 1D–I, Supplementary Fig. 2A,D, and Supplementary Table 1) (Beed et al. 2010; Canto and Witter 2012). Similarly, local application of histamine excited the pyramidal neurons (Supplementary Fig. 2B,E). Histamine (10 μM)-induced depolarization was not significantly different between stellate and pyramidal neurons in the Layer II of the MEC (stellate neurons: 3.3 ± 0.3 mV, n = 12; pyramidal neurons: 3.4 ± 0.5 mV, n=7; P=0.79; unpaired t-test; Supplementary Fig. 2C). Moreover, when recording at the somata, no significant difference was found in histamine-induced depolarization between pyramidal neurons in the Layers II and III (pyramidal neurons in Layer II: 3.4 ± 0.5 mV, n = 7; pyramidal neurons in Layer III: 3.8 ± 0.7 mV, n = 5; P = 0.67; unpaired t-test; Supplementary Fig. 2F).

EC-cortical projections primarily arise from Layer V pyramidal neurons (Canto et al. 2008). These neurons are characterized by a pyramidal or elongated soma (Supplementary Fig. 1K). Moreover, unlike the stellate neurons, they had no depolarizing voltage sags (Fig. 1E and Supplementary Table 1) and small hyperpolarization-activated currents (Supplementary Fig. 1L and Supplementary Table 1). We accordingly tested whether histamine affected the excitability of these neurons in the deep layers of the MEC. When recording at the somata, application of histamine at 10 μM failed to change the membrane potentials (control: −62.0 ± 1.6 mV; histamine: −61.8 ± 1.8 mV; n = 8; P = 0.61; paired t-test; Fig. 1F,H) and holding currents (control: −46.2 ± 11.2 pA; histamine: −46.0 ± 10.6 pA; n = 19; P = 0.94; paired t-test; Fig. 1G,I) in all the recorded pyramidal neurons from Layer V of the MEC. In addition, the membrane potentials (−60.7 ± 0.7 and −61.1 ± 0.6 mV before and during applying 100 μM histamine, n = 10, P = 0.22; −60.5 ± 0.6 and −60.9 ± 0.7 mV before and during applying 1 mM histamine, n = 10, P = 0.17; paired t-test; Fig. 1F,H) and holding currents (−32.3 ± 14.3 and −33.5 ± 14.6 pA before and during applying 100 μM histamine, n = 12, P = 0.07; −30.8 ± 12.4 and −29.9 ± 12.2 pA before and during applying 1 mM histamine, n = 13, P = 0.19; paired t-test; Fig. 1G,I) of Layer V pyramidal neurons were not affected by 100 μM and 1 mM histamine. We also investigated the effects of histamine on the interneuron excitability in the MEC. The superficial layer and deep layer interneurons have large input resistance (superficial layers: 317.2 ± 29.4 MΩ, n = 6; deep layers: 364.9 ± 51.8 MΩ, n = 7) and fast after hyperpolarization (fAHP) (superficial layers: 18.2 ± 1.5 mV, n = 6; deep layers: 17.4 ± 0.7 mV, n = 7) compared with the principal projection neurons. When recording at the somata, the membrane potentials of the interneurons in the MEC were not affected by histamine at concentrations of 10 μM (superficial layers: −63.4 ± 1.4 and −63.3 ± 1.0 mV before and during applying, n = 4, P = 0.78; deep layers: −61.3 ± 1.8 and −61.1 ± 1.4 mV before and during applying, n = 5, P = 0.66; paired t-test), 100 μM (superficial layers: −63.4 ± 0.9 and −63.6 ± 0.9

mV before and during applying, n = 5, P = 0.64; deep layers: −61.4 ± 1.3 and −61.0 ± 1.1 mV before and during applying, n = 6, P = 0.13; paired t-test), and 1 mM (superficial layers: −63.5 ± 0.9 and −63.8 ± 0.9 mV before and during applying, n = 4, P = 0.60; deep layers: −61.6 ± 1.8 and −61.0 ± 1.9 mV before and during applying, n = 6, P = 0.26; paired t-test). Together, these results suggest that histamine selectively increases excitability of principal projection neurons in the superficial, but not deep, layers of the MEC when recording at the somata. Considering the effect of histamine in the superficial layers is not cell-type specific and the axons of stellate neurons forming the perforant pathway provide the main output from the EC to the hippocampus (Alonso and Klink 1993; Canto et al. 2008), we primarily focused on the stellate neurons in the superficial layers to investigate the cellular mechanisms underlying histamine-induced excitation.

Histamine Selectively Decreases Spontaneous GABA, but Not Glutamate, Release in the Superficial, but Not Deep, Layers of the MEC

Since synaptic release is crucial for regulating individual neuronal as well as neural network excitability, it is important to know whether histamine affects synaptic transmission in the MEC. To test this, we recorded spontaneous miniature postsynaptic currents in the presence TTX (1 μM) to block voltage-gated Na^+ channels. An alteration in the amplitude of spontaneous miniature postsynaptic currents reflects a postsynaptic mechanism, whereas a change in the frequency of these currents signifies a change in the presynaptic release (Li et al. 2011).

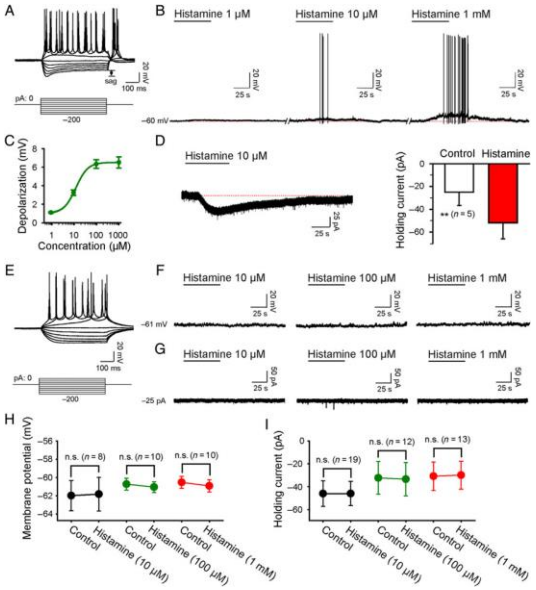

Figure 1. Histamine selectively increases the excitability of principal neurons in the superficial layers of the MEC. (A) The voltage responses generated by current injection of the stellate neuron in the MEC. Stellate neurons exhibited profound depolarizing voltage sags in response to hyperpolarizing current pulses. (B) Histamine generated membrane depolarization in a concentration-dependent manner and increased the neuronal firing rate. (C) Concentration–response curve for histamine on stellate neurons showed the mean EC_{50} of 14.2 ± 1.5 μM. (D) Local application of histamine induced an inward current in the stellate neuron (left). Summarized data for histamine (10 μM)-induced changes in holding currents of stellate neurons (right). (E) The electroresponsive membrane properties of pyramidal neurons in the Layer V of the MEC. (F, G) Histamine failed to alter the membrane potentials (F) and the holding currents (G) of the pyramidal neurons in the Layer V of the MEC. (H, I) Data for the membrane potentials (H) and holding currents (I) of the Layer V pyramidal neurons in the absence and presence of histamine. n.s., nonsignificant. *P < 0.05, **P < 0.01, and ***P < 0.001 in this and the following figures

We initially recorded the mEPSCs in the presence of $GABA_A$ receptor antagonist PIC (100 μM) at a fixed potential of −60 mV. Similar to other cortical neurons, the stellate neurons in the MEC exhibited a continuous level of fast

excitatory activities that were completely blocked by CNQX (10 μM) and AP5 (50 μM), confirming that they were mediated by ionotropic glutamate receptors (data not shown). After a stable recording, application of histamine (10 μM) did not influence the cumulative probability distributions of interevent interval (P = 0.31, K–S test, Fig. 2B, left) and amplitude (P = 0.14, K–S test, Fig. 2B, right). On average, histamine did not affect the frequency (control: 2.84 ± 0.47 Hz, histamine: 2.99 ± 0.36 Hz, washout: 2.97 ± 0.51 Hz, n = 7, P = 0.92; one-way repeated-measures ANOVA; Fig. 2C, left) and amplitude (control: 9.00 ± 0.61 pA, histamine: 8.95 ± 0.68 pA, washout: 8.74 ±0.64 pA, n = 7, P = 0.64; one-way repeated-measures ANOVA; Fig. 2C, right) of mEPSCs in 7 stellate neurons examined. Together, these data indicate that histamine does not influence the glutamatergic transmission in the superficial layers.

To study modulation of GABAA receptor-mediated mIPSCs, ionotropic glutamate receptors were blocked with CNQX (10 μM) and AP5 (50 μM). After establishing the whole-cell configuration, a period of at least 15 min was allowed for the equilibration of intracellular and recording solutions. Since the pipette recording solution contained a high concentration of CsCl (145 mM), mIPSCs were recorded from the stellate neurons as inward currents that were abolished by PIC (100 μM), indicating that these currents were mediated by GABAA receptors (data not shown). After a stable baseline was achieved, application of histamine (10 μM) reversibly suppressed the mIPSC activity (Fig. 2D) and caused a rightward shift of the interevent interval distribution of mIPSCs (P < 0.001, K–S test, Fig. 2E, left), reflecting a decrease in mIPSC frequency. However, histamine did not affect the cumulative distribution of mIPSC amplitude (P = 0.34, K–S test, Fig. 2E, right). There was a group difference in the frequency of mIPSCs (control: 2.13 ± 0.34 Hz, histamine: 1.43 ± 0.24 Hz, washout: 1.93 ±0.36 Hz, n = 7, P < 0.01; one-way repeated-measures ANOVA; Fig. 2F, left). LSD post hoc comparisons revealed that the frequency of mIPSCs was decreased to 67 ± 11% of control after application of histamine (P < 0.001, Fig. 2F, left). Application of histamine did not affect the mIPSC amplitude (control: 21.30 ± 1.62 pA, histamine: 21.80 ± 2.34 pA, washout: 22.49 ± 2.78 pA, n = 7, P = 0.62; one-way repeated-measures ANOVA; Fig. 2F, right). Together, these findings suggest that histamine selectively inhibits GABAergic synaptic transmission in the superficial layers of the MEC.

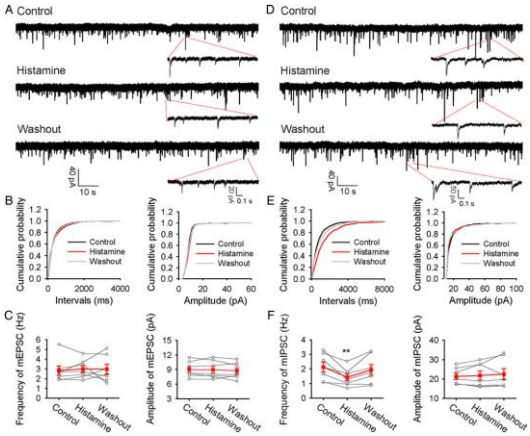

Figure 2. Histamine decreases spontaneous GABA release on to stellate neurons in the superficial layers of the MEC, whereas it does not affect the glutamatergic transmission. (A, D) Typical traces of miniature excitatory postsynaptic currents (mEPSCs) (A) and inhibitory postsynaptic currents (mIPSCs) (D) observed before, during, and after the application of 10 μM histamine. (B) Cumulative probability curves for interevent interval and amplitude distribution of

mEPSCs were similar before, during, and after histamine application. (C) Graphs depicting the individual (open circle) and average (closed squares) mEPSC frequency (left) and amplitude (right) before, during, and after the application of histamine. (E) Histamine induced a rightward shift of the mIPSC interevent interval cumulative distribution curve, whereas it had no effect on its amplitude distribution. (F) Graphs depicting the individual (open circle) and average (closed squares) mIPSC frequency (left) and amplitude (right) before, during, and after the application of histamine, noting that histamine reduced the frequency of the mIPSCs.

We also investigated the effect of histamine on the synaptic release on to the pyramidal neurons in the Layer V of the MEC. The protocols used for isolating the mEPSCs and mIPSCs are the same as those mentioned above. Application of histamine had no impact on the shape of mEPSC or mIPSC cumulative probability curves of interevent intervals (mEPSCs: $P = 0.50$; mIPSCs: $P = 0.59$; K–S test; Fig. 3B,E) and event amplitudes (mEPSCs: $P = 0.42$; mIPSCs: $P = 0.43$; K–S test; Fig. 3B,E), respectively. Histamine did not affect the frequency (control: 1.36 ± 0.23 Hz, histamine: 1.24±0.25Hz, washout: 1.23±0.22Hz, $n = 9$, $P = 0.39$; one-way repeated-measures ANOVA; Fig. 3C, left) and amplitude (control: 13.90 ± 1.37 pA, histamine: 14.06 ± 1.31 pA, washout: 13.90 ± 1.49 pA, $n = 9$, $P = 0.98$; one-way repeated-measures ANOVA; Fig. 3C, right) of mEPSCs in 9 pyramidal neurons examined. Similarly, the frequency (control: 2.24 ± 0.36 Hz, histamine: 2.27 ± 0.24 Hz, washout: 2.15 ± 0.26 Hz, n = 7, P = 0.84; one-way repeated-measures ANOVA; Fig. 3F, left) and amplitude (control: 31.50 ± 3.05 pA, histamine: 31.91 ± 2.85 pA, washout: 32.60 ± 3.74 pA, $n = 7$, $P = 0.86$; one-way repeated-measures ANOVA; Fig. 3F, right) of mIPSCs were unaffected by histamine. Together, these results imply that histamine selectively modulates the GABAergic, but not glutamatergic, synaptic transmission in a superficial layer-specific manner.

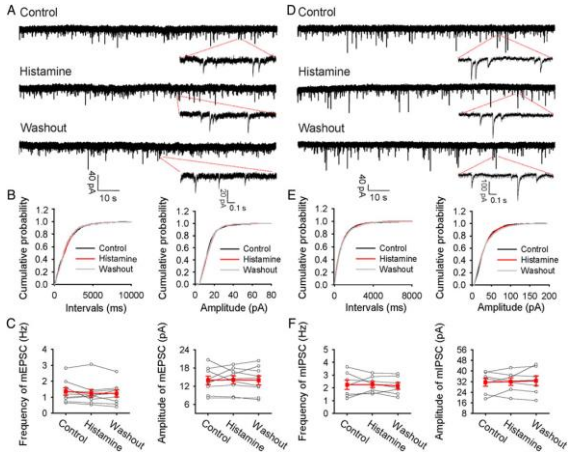

Figure 3. Histamine does not affect the synaptic release on to pyramidal neurons in the deep layers of the MEC. (A, D) Typical traces of mEPSCs (A) and mIPSCs (D) recorded before, during, and after the application of 10 μM histamine. (B, E) Cumulative probability curves for interevent interval (left) and amplitude (right) distribution of mEPSCs (B) and mIPSCs (E) were similar before and during histamine application. (C, F) Graphs depicting the individual (open circle) and average (closed squares) mEPSC (C) and mIPSC (F) frequency (left) and amplitude (right) before, during, and after the application of histamine, noting that histamine did not influence the GABA and glutamate release on to the pyramidal neurons in the deep layers of the MEC.

Histamine-Induced Depolarization in the Superficial Layers Is Mediated by H_1R-Dependent Inhibition of Kir Channels

The actions of histamine are mediated via 3 distinct types of G-protein-coupled receptors (H_1Rs, H_2Rs, and H_3Rs) in the CNS. H_1Rs and H_2Rs are postsynaptically coupled to Gq/11 and Gs proteins, respectively, whereas H_3Rs, coupled to Gi/o protein, are preferentially located at presynaptic terminals acting as auto-or heteroreceptors to modulate the release of a number of neurotransmitters (Arrang et al. 2007;

Haas et al. 2008; Passani and Blandina 2011). Here, the receptor mechanism underlying the direct excitatory action of histamine was determined by using histamine receptor-selective antagonists. The effects of histamine blocked by these antagonists can be always mimicked by the corresponding histamine receptor agonists (Zhou et al. 2006; Dai et al. 2007; Lundius et al. 2010). In the presence of triprolidine (2 μM), a selective H_1R antagonist, the histamine (10 μM)-elicited depolarization on stellate was abolished (3.0 ± 0.7 and 0.1 ± 0.1 mV before and after applying triprolidine, n = 5, P < 0.05; paired t-test; Fig. 4A). However, application of H_2R blocker ranitidine (30 μM) failed to alter histamine (10 μM)-induced membrane depolarization in stellate neurons (3.4 ± 0.2 and 3.1 ± 0.2 mV before and after applying ranitidine, n = 8, P = 0.32; paired t-test; Fig. 4B). Neither did application of clobenpropit (400 nM), a selective H_3R antagonist, significantly change histamine (10 μM)- elicited membrane depolarization (3.5 ± 0.2 and 3.4 ± 0.2 mV before and after applying clobenpropit, n = 4, P = 0.59; paired t-test; Fig. 4C). Consistent with this, the results of immunofluorescence reveal that H_1Rs were expressed at the cell bodies and dendritic processes of principal neurons in the superficial layers, but not in deep layers, of the MEC (Fig. 4D–F) whereas the distribution of H_2Rs in the superficial layers and deep layers of the MEC was relative scarce compared with H_1Rs (Supplementary Fig. 3A–C). Together, these results provide direct electrophysiological and morphological evidence that histamine depolarizes the stellate neurons in the superficial layers of the MEC by activation of H_1Rs.

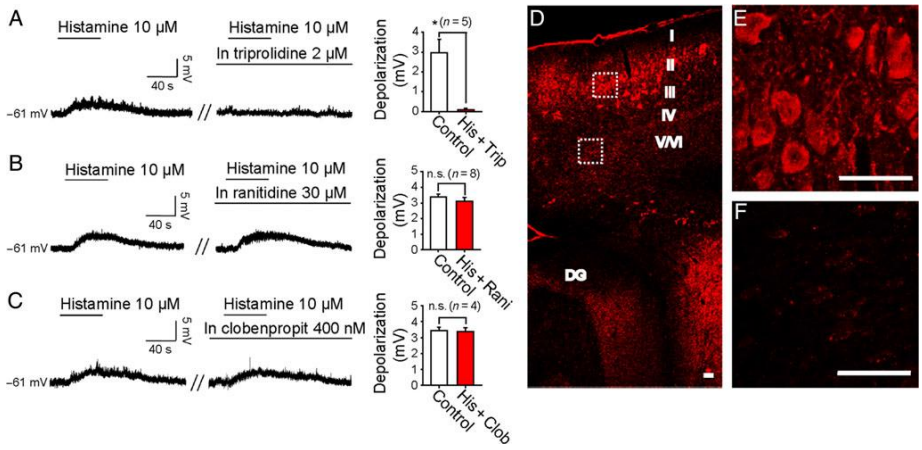

Figure 4. Histamine depolarizes the stellate neurons via activation of H_1Rs. (A) Selective H_1R antagonist triprolidine (2 μM) abolished the histamine-induced depolarization on stellate neurons. (B) The depolarization induced by histamine was similar in the absence or presence of selective H_2R antagonist ranitidine (30 μM). (C) The depolarization induced by histamine was similar in the absence or presence of selective H_3R antagonist clobenpropit (400 nM). (D) Antibody staining for H_1Rs in the rat EC. Note that H_1R immunostainings particularly enriched in the neuronal soma and dendrites in the superficial layers of the MEC. (E, F) Expanded views of the regions indicated by the dashed frames in the Layer II (E) and V (F). Scale bars: 50 μm.

To clarify the ionic mechanisms underlying the histamine-induced depolarization in stellate neurons, we first tested whether the histamine-induced depolarization was a direct postsynaptic effect. Histamine (10 μM)-induced depolarization persisted in the presence of either TTX (1 μM) (3.6 ± 0.6 and 3.3 ± 0.5 mV before and after applying TTX, n = 5, P = 0.81; paired t-test; Supplementary Fig. 4A) or CNQX (10 μM), AP5 (50 μM), and PIC (100 μM) (3.5 ± 0.3 and 3.2 ± 0.4 mV before and after applying, n = 5, P = 0.38; paired t-test; Supplementary Fig. 4B) known to block synaptic transmission, thus indicating that the action of histamine is postsynaptic. Moreover, input conductance was determined before and after the application of histamine using a series of hyperpolarized voltage pulses. Accompanying the histamine-induced depolarization, 0.6 nS, n = 4, P < 0.05; paired t-test; Supplementary Fig. 4C), suggesting that histamine causes a closure of ion channels on the postsynaptic membrane.

To test whether the effect of histamine would result from the closure of a potassium conductance, we conducted slow ramp command tests (dV/dt = –10 mV/s) to evaluate the I–V curves for a large voltage range in the absence and presence of histamine. In an ACSF with K_0 at 3mM (estimated the theoretical K^+ reversal potential by the Nernst equation: E_k = –88.59 mV), comparing voltage-clamp ramps in control and in the presence of histamine indicated a reversal of the histamine effect of approximately −90 mV (Fig. 5A). In 7 neurons, the mean (± SEM) reversal potential was −87 ± 1 mV, thus very close to the estimated E_k (Fig. 5D). Performing the same experiment in an ACSF with K_0 at 10 mM (estimated E_k = −58.17 mV) indicated a reversal of the histamine effect of approximately −60 mV (Fig. 5C). In 4 cells, the mean reversal was now −59 ± 1 mV, thus again very close to the estimated E_k (Fig. 5D). Thus, these results indicate that the action of histamine on the stellate neurons in the MEC is mediated through the closure of a potassium conductance. Subtracting the control from the current recorded during histamine application yielded a difference current representing the histamine-induced current. The difference current obtained from the 7 stellate neurons in normal ACSF exhibited a strong inward rectification (Fig. 5B), indicating that the potassium channels inhibited by histamine are inwardly rectifying K^+ (Kir) channels.

Next, we applied the classic K^+ channel blockers to identify the properties of the involved K^+ channels. Histamine (10 μM)-induced depolarization in stellate neurons was not significantly altered in the extracellular solution containing 2 mM 4AP (control: 3.1 ± 0.2 mV; 4AP: 3.0 ± 0.3 mV; n = 6; P = 0.77; paired t-test; Fig. 5G,I) or 10mM TEA (control: 3.2 ± 0.8 mV; TEA: 3.3 ± 0.8 mV; n = 4; P = 0.89; paired t-test; Fig. 5H,I), suggesting that histamine-induced excitation is insensitive to the voltage-dependent potassium channel blockers. Since Kir channels are sensitive to Ba^{2+} (Hibino et al. 2010), we therefore tested the role of Ba^{2+} in histamine-induced membrane depolarization. Inclusion of Ba^{2+} (2mM) in the extracellular solution induced membrane depolarization. After the baseline stabilized, application of histamine (10 μM) failed to elicit membrane depolarization (control: 3.2 ± 0.5 mV; Ba^{2+}: 0.3 ± 0.2mV; n = 6; P < 0.01; paired t-test; Fig. 5E,I). Considering some of two-pore-domain potassium channels are sensitive to Ba^{2+} (Deng et al. 2009; Xiao et al. 2009), we therefore tested the role of another Kir channel blocker Cs^+, which has no effect on the two-pore-domain potassium channels. In the

presence of Cs^+ (3 mM), histamine (10 μM)-elicited membrane depolarization was also almost completely blocked (control: 3.1 ± 0.5 mV; Cs^+: 0.1 ± 0.3 mV; n = 5; P < 0.01; paired t-test; Fig. 5F,I). Together, these results indicate that histamine-induced membrane depolarization is mediated by Kir channels, but not by two-pore-domain potassium channels.

H_1Rs are coupled to $G_{q/11}$ protein to activate protein kinase C (PKC) signaling pathway (Passani and Blandina 2011). We next determined the role of PKC in histamine-induced depolarization. After bath incubation with PKC inhibitor BIS-II (500 nM) at least for 90 min, the effect of histamine on stellate neurons in the MEC was blocked (Supplementary Fig. 5A). The histamine-elicited depolarization was significantly reduced to 7.0 ± 4.2% of control (control: 3.3 ± 0.3 mV, n = 12; BIS-II: 0.23 ± 0.14 mV, n = 10; P < 0.001; unpaired t-test; Supplementary Fig. 5B) in the presence of BIS-II. Furthermore, histamine failed to induce an inward current in the slow ramp command tests (Supplementary Fig. 5C). These results together demonstrate that the activation of PKC is necessary for histamine-induced excitation.

Inhibition of Spontaneous GABA Release by Histamine in the Superficial Layers Requires H_3R-Dependent Modulation of the VGCCs

Next, we investigated the histamine receptor subtype involved in the regulation of inhibitory synaptic transmission. In this set of experiments, we first added triprolidine (2 μM), ranitidine (30 μM), or clobenpropit (400 nM)) into the bathing solution after a stable baseline recording and then the histamine (10 μM) was superfused. Neither triprolidine nor ranitidine changed the histamine-induced shift of the interevent interval distribution (triprolidine: P < 0.001; ranitidine: P < 0.001; K–S test; Fig. 6B,D). There was a significant group difference in the frequency of mIPSCs for the triprolidine (control: 2.05 ± 0.24 Hz, triprolidine: 1.91 ± 0.25 Hz, histamine + triprolidine: 1.31 ± 0.19 Hz, washout: 1.63 ± 0.36 Hz, n = 6, P < 0.05, one-way repeated-measures ANOVA on ranks, Fig. 6A,B)-or ranitidine (control: 1.97 ± 0.41 Hz, ranitidine: 2.14 ± 0.52 Hz, histamine + ranitidine: 1.26 ± 0.24 Hz, washout: 1.81 ± 0.37 Hz, n = 7, P < 0.05, one-way repeated-measures ANOVA, Fig. 6C,D)-treated experiments. Post hoc comparisons revealed that application of histamine still reduced the mIPSC frequency in the presence of triprolidine (P < 0.05, Dunn's test, Fig. 6A,B) or ranitidine (P < 0.05, LSD test, Fig. 6C,D). However, histamine-mediated decrease in the frequency of mIPSCs was blocked by H_3R antagonist clobenpropit (control: 2.61 ± 0.55 Hz, clobenpropit: 2.56 ± 0.45 Hz, histamine + clobenpropit: 2.85 ± 0.65 Hz, washout: 2.76 ± 0.30 Hz, n = 6, P = 0.68; one-way repeated-measures ANOVA; Fig. 6E,F). These electrophysiological results suggest that the histamine-induced decrease in spontaneous GABA release is mediated by presynaptic H_3Rs.

To better understand the role of H_3Rs in regulating GABAergic transmission, we analyzed the receptor's colocalization with the well-known marker of GABAergic terminals, GABA-synthesizing enzyme glutamic acid decarboxylase (67 kDa form, GAD-67). In the superficial layers of the MEC, double labeling for H_3Rs and GAD-67 revealed widespread colocalization (Supplementary Fig. 6A1–A3). At higher magnification, the colocalization was always observed on the inhibitory synaptic terminals that contact with the putative principal projection neuron bodies and the GABAergic

neuron soma (Fig. 6G1–G3, H1–H3). Instead, the expression level of H_3Rs in the deep layers of the MEC was relatively low compared with that in the superficial layers (Supplementary Fig. 6A1–A3). Double staining with H_3Rs/GAD-67 showed scarce colocalization in the deep layers (Supplementary Fig. 6B1–B3 and C1–C3). GAD-67 mainly labeled inhibitory terminals that rarely expressed H_3Rs. Overall, these morphological results combined with the electrophysiological data imply that histamine presynaptically suppresses GABA release in the superficial layers of the MEC by stimulating the H_3Rs.

Recent studies suggest that spontaneous synaptic release depends on Ca^{2+} entry via voltage-gated Ca^{2+} channels (VGCCs) (Dawet al. 2009; Groffen et al. 2010).We therefore tested whether the histamine-elicited decrease in mIPSC frequency was VGCC dependent. Bath application of Cd^{2+} (100 μM), a general VGCC blocker, alone induced a rightward shift of the interevent interval distribution of mIPSCs (P<0.001,K–S test, Fig. 7A) and significantly decreased the frequency to 57 ± 6% of control (control: 2.37 ± 0.22 Hz, Cd^{2+}: 1.37 ± 0.15 Hz, histamine + Cd^{2+}: 1.30 ± 0.25 Hz, n=7, control vs. Cd^{2+}: P < 0.01; LSD post hoc comparisons following one-way repeated-measures ANOVA; Fig. 7A). These results imply that activation of VGCCs contributes to the generation of mIPSCs. After at least 6-min pretreatment of Cd^{2+}, application of histamine failed to alter the frequency of mIPSCs (n = 7, P = 0.80; LSD post hoc comparisons following one-way repeated-measures ANOVA; Fig. 7A), indicating that the inhibitory effect of histamine on GABA release is mediated by VGCCs. Moreover, application of histamine did not induce a significant change in the frequency of mIPSCs in Ca^{2+}-free external solution (control: 2.47 ± 0.55 Hz, Ca^{2+}-free: 1.46 ± 0.37 Hz, histamine + Ca^{2+}-free: 1.30 ± 0.27 Hz, n = 5, Ca^{2+}-free vs. histamine + Ca^{2+}-free: P = 0.65; LSD post hoc comparisons following one-way repeated-measures ANOVA; Fig. 7B). Together, these results suggest that H_3R-induced inhibition of spontaneous GABA release depends on extracellular Ca^{2+} passing through the VGCCs.

Histamine Increases the Sensitivities of Stellate Neurons to a Depolarizing Ramp-Like Current Stimulation

Given that histamine inhibits Kir channels and GABA release in the superficial layers, we asked whether these effects affect the firing properties and sensitivity of stellate neurons to a depolarizing ramp-like current stimulation (Fig. 8A), consisting of a 600-ms ramp (−150 to 150 pA, slope of 0.5 nA/s) followed by a long plateau of current (150 pA, 4400 ms). The initial membrane potentials of neurons were set at the similar level before and during the application of histamine. Application of histamine (10 μM) remarkably shortened the first-spike latency from 582.6 ± 18.8 to 524.1 ± 19.3 ms (n = 9; P < 0.01; paired t-test; Fig. 8A, B and D). Moreover, histamine increased the instantaneous firing rate (Fig. 8A, B) of the stellate neurons from 13.3 ± 2.5 spikes/s to 16.2 ± 3.0 spikes/s (n = 5; P < 0.05; paired t-test; Fig. 8C) during 150 pA current injection, implying an increase in the neuronal sensitivity to the current stimulation. However, histamine did not affect (control: 7.3 ± 2.1 spikes/s; histamine: 7.7 ± 3.5 spikes/s, n = 5; P = 0.87; paired t-test; Fig. 8E) the difference between the instantaneous firing rate at the end of the ramp and the stable discharge rate at the end of the plateau (firing frequency adaptation in spikes/s; Fig. 8E). Thus, histamine did not

change the firing frequency adaptation. The increase in both the firing rate and sensitivity of stellate neurons implies that the histaminergic afferent system in the superficial layers of the MEC may have a physiological function.

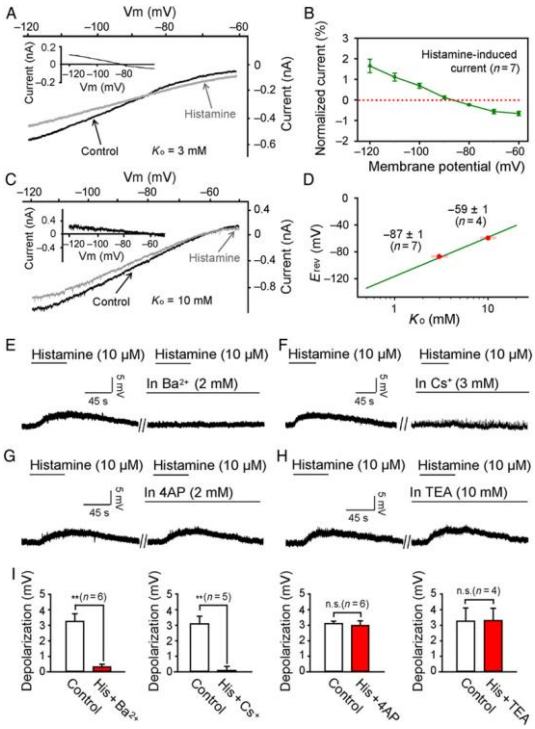

Figure 5. Histamine-induced depolarization is mediated by the inhibition of Kir channels and requires the activation of PKC. (A) Voltage-clamp ramps in the absence or presence of histamine (10 μM) with K_0 at 3 mM in ACSF. Inset, subtraction of the current prior to the application of histamine generated a net current of inward rectification. (B) The difference current obtained from the 7 stellate neurons in an ACSF with K_0 at 3 mM. Histamine-induced current exhibited strong inward rectification. (C) Voltage-clamp ramps in the absence or presence of histamine (10 μM) with K_0 at 10mM in ACSF. Inset, subtraction of the current prior to the application of histamine revealed a net current. (D) Reversal potentials for both conditions with respect to Nernst relationship. (E, F) Histamine-induced membrane depolarization was blocked by extracellular Ba^{2+} (2 mM) or Cs^+ (3 mM). (G, H) Histamine-induced excitation was insensitive to the voltage-dependent potassium channel blockers 4AP (2 mM) or TEA (10mM). (I) Summary histogram illustrating the pharmacological profile of histamine-induced depolarization in the presence of different potassium channel blockers.

Blockade of H_1Rs or H_3Rs in the Superficial, but Not Deep, Layers of the MEC Impairs Rat Spatial Learning in Morris Water Maze

Because of the key role of the MEC in spatial navigation, we asked whether the excitatory effect of histamine on the principal neurons would influence spatial learning. In this set of experiments, we first implanted cannula into the superficial layers of the MEC and tested effects of histamine receptor antagonists in this region on rat spatial learning in Morris water maze. Rats receiving sham-operation (n = 14) or intrasuperficial layer infusion of ACSF (n = 14), triprolidine (n = 9), ranitidine (n = 14), and clobenpropit (n = 11) showed a reduction in escape latencies to find the hidden platform throughout the trials in water maze tasks as two-way repeated-measures ANOVA revealed a significant main effect of trial ($F_{11, 627}$ = 19.67; P < 0.001; Fig. 9A) and no groups-by-trials interaction ($F_{44, 627}$ = 1.33; P = 0.08; Fig. 9A). Analysis of the latency traveled to the escape platform during training revealed a significant main effect of group ($F_{4, 57}$ = 7.61; P < 0.001; two-way repeated-measures ANOVA; Fig. 9A). LSD post hoc comparisons revealed that the rats receiving intrasuperficial layer infusion of triprolidine or clobenpropit had longer escape latencies than the ACSF-treated group (triprolidine: P < 0.001; clobenpropit: P<0.01), indicating that blockade of either H_1Rs or H_3Rs in the superficial layers of the MEC impairs rat spatial learning. Conversely, microinjection of the H_2R antagonist ranitidine failed to alter the escape latencies compared with the ACSF-treated group (P = 0.86). In the probe trials, rats treated with ACSF and

ranitidine showed a significant bias for the target quadrant where the platform had been originally located ($P < 0.05$ for each group compared with the chance level 25%, one-sample *t*-test, Fig 9C). However, rats receiving triprolidine or clobenpropit failed to show preference for the target quadrant (triprolidine: $P = 0.08$; clobenpropit: $P = 0.18$; one-sample *t*-test; Fig. 9C). Together, these results suggest that the activation of H_1Rs and H_3Rs by endogenous histamine in the superficial layers of the MEC contributes to spatial learning.

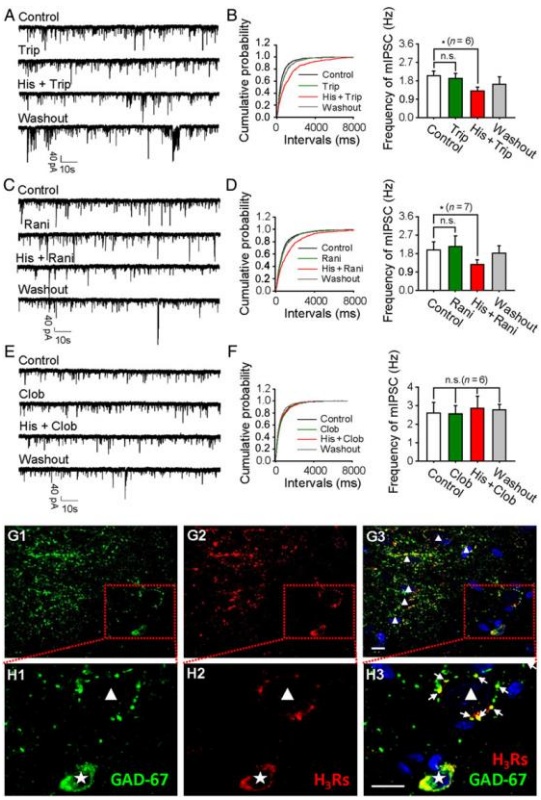

Figure 6. The inhibition of presynaptic GABA release on to stellate neurons by histamine is mediated by H_3Rs. (A, C) Sample traces of mIPSCs observed before, during, and after the application of 10 μM histamine in the absence and presence of the triprolidine (2 μM) (A) and ranitidine (30 μM) (C). (B, D) Summarized data for effects of histamine on the mIPSC interevent interval distribution (left) and frequency (right) in the absence and presence of the triprolidine (B) and ranitidine (D), noting that the inhibition of presynaptic GABA release by histamine is independent of H_1Rs and H_2Rs. (E) Sample traces of mIPSCs observed before and during the application of 10 μM histamine in the absence and presence of the clobenpropit (400 nM). (F) Summarized data for effects of histamine on the mIPSC interevent interval distribution (left) and frequency (right) in the absence and presence of the clobenpropit. Note that histamine-induced decrease in the frequency of mIPSCs was specially blocked by the H_3R antagonist clobenpropit. (G1–G3) In the superficial layers of the MEC, double immunostainings for H_3Rs and GAD-67 revealed widespread colocalization. (H1–H3) At higher magnification, the colocalization (indicated by the white arrows) was always observed on the inhibitory synaptic terminals that contact with the putative principal neuron bodies (marked by the triangle) and the GABAergic neuron soma (marked by the star). Scale bars: 10 μm.

Nonspatial learning factors, such as the motivational, emotional, and motor functions of the tested subjects, have been reported to influence the water maze performance. Thus, we took the following measures to ensure that the effects of drugs were not generated by nonspatial learning factors. First, we analyzed the recorded swimming speed of the rats. Intrasuperficial layer application of the drugs did not alter the swimming speed of the rats compared with sham-operated group ($F_{4, 57} = 0.99$; $P = 0.42$; two-way repeated-measures ANOVA; Supplementary Fig. 7A). Second, we conducted the open-field test. Both spontaneous locomotor ($F_{4, 33} = 0.59$; $P = 0.68$; one-way ANOVA; Fig. 9E) and exploratory activity ($F_{4, 33} = 0.23$; $P = 0.92$; one-way ANOVA; Fig. 9E) of rats in an open field were not affected by microinjecting ACSF ($n = 7$), triprolidine ($n = 6$), ranitidine ($n = 6$), and clobenpropit ($n = 6$) into the superficial layers of the MEC compared with sham-operated group ($n = 9$). The microinjection site was located within the superficial layers of the MEC (Fig. 9G). Thus, these results demonstrate

that either triprolidine or clobenpropit specifically affects the spatial learning rather than as a secondary effect on a motivational, emotional, or motor functions.

We also microinjected histamine receptor antagonists into the deep layers of the MEC and investigated their effects on rat spatial learning. Sham-operated (n = 10) or intradeep layer infusion of ACSF (n = 9), triprolidine (n = 11), ranitidine (n = 12), and clobenpropit (n = 7) groups exhibited a significant trial effect ($F_{11,\ 484}$ = 13.20; P < 0.001; two-way repeated-measures ANOVA; Fig. 9B), showing some improvement by both groups over the trials. However, there was no overall group difference in escape latencies to find the hidden platform ($F_{4,\ 44}$ = 1.19; P = 0.33; two-way repeated-measures ANOVA; Fig. 9B) and no groups-by-trials interaction ($F_{44,\ 484}$ = 0.60; P = 0.98; two-way repeated-measures ANOVA; Fig. 9B), reflecting the equivalent improvement of both groups across the acquisition stage.

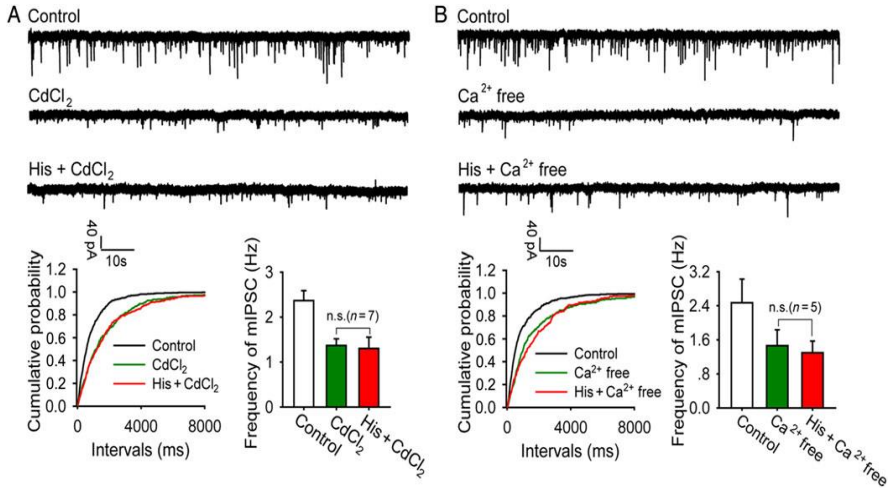

Figure 7. The inhibition of presynaptic GABA release by histamine depends on the voltage-gated Ca^{2+} channels and extracellular Ca^{2+}. (A) Representative traces show mIPSCs during control and application of 100 μM $CdCl_2$ (top plane). Summaries of the effects of histamine on the mIPSC interevent interval distribution (left) and frequency (right) in either presence of 100 μM $CdCl_2$ (bottom plane). (B) Representative traces showed mIPSCs during control and application of Ca^{2+}-free solution (top plane). Summaries of the effects of histamine on the mIPSC interevent interval distribution (left) and frequency (right) in either presence of Ca^{2+}-free solution (bottom plane).

In the probe trials, sham-operated, ACSF-, and histamine receptor antagonist-treated groups exhibited a remarkable bias for the target quadrant where the platform had been originally located (P < 0.05 for each group, one-sample t-test, Fig 9D). The placement of cannulation was confirmed at the end of the behavior study (Fig. 9H). Together, these results indicate that central histaminergic system in the deep layers of the MEC does not impact the learning phase, which is consistent with the electrophysiological results. Similar to the findings in the superficial layers, intradeep layer infusion of the drugs did not affect the swimming speed of the rats ($F_{4,\ 44}$ = 1.38; P = 0.26; two-way repeated-measures ANOVA; Supplementary Fig. 7B). Also, the spontaneous locomotor ($F_{4,\ 34}$ = 0.27; P = 0.90; one-way ANOVA; Fig. 9F) and exploratory

activity ($F_{4, 34}$ = 0.10; P = 0.98; one-way ANOVA; Fig. 9F) of rats in an open field were not affected by microinjecting ACSF (n = 6), triprolidine (n = 8), ranitidine (n = 6), and clobenpropit (n = 8) into the deep layers of the MEC compared with sham-operated group (n = 7).

Discussion

Histamine exerts neuromodulatory roles and is implicated in the regulation of several pathological/physiological processes including spatial learning and memory (Masuoka et al. 2007; Haas et al. 2008; Alvarez 2009; Zlomuzica et al. 2009). In this study, our results demonstrate that the activation of H_1Rs and H_3Rs by histamine increases the excitability of principal neurons in the superficial layers, but not deep layers, of the MEC through direct and indirect mechanisms when recording at the somata. Moreover, pharmacological blockade of the H_1Rs or H_3Rs in the superficial, but not deep, layers of the MEC specifically impaired rat spatial performance in water maze. Therefore, these data provide novel mechanisms whereby histamine selectively modulates activity of superficial layer principal neurons that mediate the functional interaction between hippocampus and other cortical regions and thereby influences the neocortex–EC– hippocampus memory circuit.

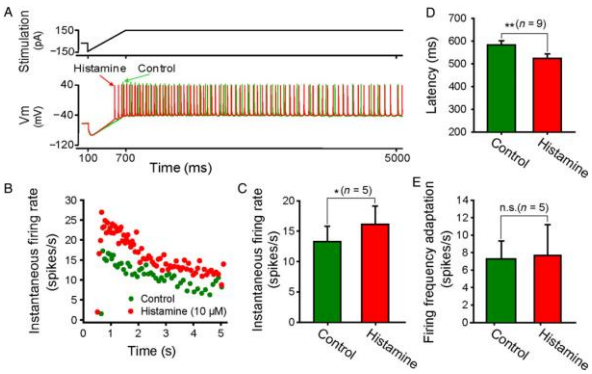

Figure 8. Histamine increases sensitivities of the stellate neurons to a depolarizing ramp-like current stimulation. (A) A ramp-like current was given from a hyperpolarized level of –150 pA for 600 ms to reach 150 pA, with the final steady-state value of 150 pA lasting 4400 ms (top). Histamine (10 μM) (red line) significantly shortened the first-spike latency of a stellate neuron to the ramp-like current (bottom). (B) Instantaneous firing rates of the same stellate neuron to the ramp-like current in the absence and presence of histamine showed that histamine significantly increases the instantaneous firing rate (spikes/s) but did not influence the firing frequency adaptation, suggesting an increase of sensitivity and unchanged dynamic property of stellate neurons by histamine. (C, D, E) Summary histograms of the tested stellate neurons.

Histaminergic neurons in the TMN are thought to play a crucial role in the maintenance of arousal state and cortical activation (Lin, Anaclet, et al. 2011; Lin, Sergeeva, et al. 2011). Pharmacologic inhibition or genetic knockout of histidine decarboxylase, the enzyme responsible for biosynthesis of histamine, inhibited the cortical activation and caused somnolence and exploratory behavioral deficits. In contrast, increased histamine level by suppression of its degradation can promote wakefulness (Monti 1993; Lin 2000; Parmentier et al. 2002). Since histaminergic varicosities have been shown to seldom make synapses (Takagi et al. 1986; Ellender et al. 2011) and currently no specific transporter for histamine has been identified (Haas and Panula 2003), histamine is thought to have widespread influence on neuronal activity possible via volume transmission. The EC, particularly its superficial layers, is innervated by densely histaminergic fibers (Steinbusch 1991; Panula et al. 1998). The present finding of excitatory effect for histamine in the MEC combined with previous anatomical results suggests that histamine signaling directly contributes to entorhinal arousal.

Mechanisms Underlying a Direct Effect of Histamine

Kir channels that govern the resting membrane potential are considered to be critically involved in the regulation of the neuronal excitability (Hibino et al. 2010). Our results reveal that histamine directly modulates the excitability of entorhinal neurons, particularly the stellate neurons, in the superficial layers by inhibiting Kir channels based on the following bodies of evidence. First, the net current induced by histamine had a reversal potential close to the K^+ reversal potential. Second, the difference current obtained from the stellate neurons exhibited strong inward rectification, which is one of the most important features of Kir channels. Third, we have shown that the histamine-elicited depolarization is blocked by either Ba^{2+} or Cs^+, both of which are most commonly used blockers for Kir channels (Hagiwara et al. 1976; Hagiwara et al. 1978; French and Shoukimas 1985) and insensitive to voltage-dependent potassium channels blockers TEA or 4AP. Whereas Ba^{2+} blocks some of two-pore-domain potassium channels that are also involved in controlling resting membrane potential (Deng et al. 2009; Xiao et al. 2009), the two-pore-domain potassium channels are unlikely to be the targets for histamine in the MEC based on the following 2 lines of evidence. First, the two-pore-domain potassium channels are insensitive to extracellular Cs^+ whereas application of this classic K^+ channel blocker abolished the histamine-induced depolarization. Second, the two-pore-domain potassium channel-mediated current does not exhibit strong inward rectification.

To the best of our knowledge, our results for the first time reveal that the observed effects of histamine on neurons are mediated primarily through the inhibition of Kir channels. Kir channels are shut down during membrane depolarization and open to accelerate repolarization (Nishida and MacKinnon 2002; Day et al. 2005; Hibino et al. 2010). Therefore, the inhibition of Kir channels by histamine can not only cause a depolarization of membrane potential and increase firing rate but also delay repolarization that consequently enhances sensitivity of stellate neurons to ramp-like current stimulation.

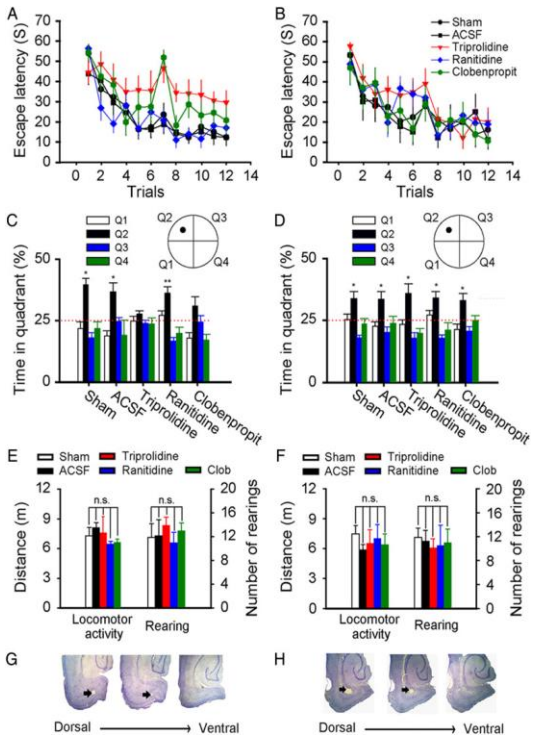

Figure 9. Pharmacological blockade of H_1Rs or H_3Rs in the superficial, but not deep, layers of the MEC specifically impairs spatial learning in Morris water maze. (A) The summarized data for the latencies to find the hidden platform across the 6 acquisition trials of a day, noting that microinjection of H_1R or H_3R antagonist into the superficial layers of the MEC had longer escape latencies than the sham-operated group and ACSF-treated group. (C) Mean percentage of time for each group spent in each of the 4 quadrants during the probe trial (*$P < 0.05$ and **$P < 0.01$ vs. 25% chance in each quadrant). (E) Intrasuperficial layer infusion of histamine receptor antagonists did not affect the

spontaneous locomotor and exploratory activities of rats in an open field. (G) Horizontal brain sections from the dorsal to ventral illustrating the microinjection site indicated by the black arrows were located within the superficial layers of the MEC. (B, D, F, H) Data from the deep layers were arranged in the same way, noting that microinjection of histamine receptor antagonists into the deep layers of the MEC failed to alter the spatial learning, locomotor, and exploratory activities of rats.

In the MEC, histamine-elicited depolarization was blocked by the potent and selective H_1R, but not H_2R or H_3R, antagonist. Furthermore, immunochemical results in this study confirmed that there is a high density of H_1Rs in the superficial, but not the deep, layers. Combined with the findings of low expression of H_2Rs in the MEC, these results suggest that a greater number of H_1R-mediated postsynaptic responses would be observed. The activation of H_1Rs can excite neurons in cortex and hippocampus by the activation of PKC (Haas et al. 2008). Consistent with the previous findings, our results indicate that PKC is necessary for direct action of histamine in the MEC. Phosphorylation of the Ser residues in Kir2.1 and Kir2.3 by PKC has been showed to suppress the channel activity (Henry et al. 1996; Tang et al. 1999; Karle et al. 2002). Considering the fact that Kir2 mRNA are highly expressed in EC (Karschin et al. 1996), the most plausible mechanism for blockade of PKC to attenuate histamine-induced depolarization is the direct interaction between PKC and Kir channels. However, it still cannot rule out the possibility that PKC modulates Kir channels via an intermediary. Overall, the postsynaptic effect of 10 μM histamine in the superficial layers is primarily mediated by the H_1Rs–PKC signaling pathway. Previous study found that histamine affected hippocampal excitatory postsynaptic potentials via an unknown mechanism when a slight shift of the pH in the acidic direction (Yanovsky et al. 1995). At a few occasions, we puffed 100 μM and 1mM histamine onto slices to investigate its postsynaptic effects. Although the histamine was puffed and can be further diluted in the bath groove, the present study cannot exclude the possibility that the proton concentration might be slightly altered at these high concentrations, thus causing unspecific effect.

Mechanisms of Histamine-Induced Suppression of Presynaptic GABA Release

Our results showed that histamine suppresses GAB Aergic, but not glutamatergic, transmission in the superficial layers of the MEC by decreasing presynaptic GABA release without altering postsynaptic $GABA_A$ receptors because histamine only decreased the frequency without altering the amplitude of mIPSCs. Interestingly, the indirect action of histamine was also superficial layer-specific since application of histamine did not affect the synaptic release on to the pyramidal neurons in the deep layers. In the MEC, histamine-induced suppression of presynaptic GABA release was specifically blocked by the H_3R antagonist. Furthermore, staining of immunofluorescence revealed that H_3Rs were mainly expressed in the superficial layers of the MEC and preferentially colocalized with the GAD-67-labeled inhibitory terminals. Overall, these data indicate that histamine inhibited the GABAergic input to stellate neurons via H_3Rs, which is in agreement with earlier reports indicating that H_3Rs preferentially act as heteroreceptors at presynaptic terminals and constrain the release of various transmitters including the GABA (Garcia et al. 1997; Drutel et al. 2001; Bergquist et al. 2006; Ellender et al. 2011; Passani and Blandina 2011). To further strengthen our

conclusions, future studies are needed to detect whether the H_3Rs are specifically expressed at the axonal terminals of the superficial GABAergic neurons by using immunoelectron microscopy.

The presynaptic VGCCs are important targets for various neuromodulators to influence the synaptic release (Huang et al. 2011; Li et al. 2011). In these experiments, blockade of VGCCs or removing extracellular Ca^{2+} profoundly reduced the inhibiting effect of histamine on mIPSCs, implying that modulation of VGCCs by H_3Rs is likely to contribute to the inhibition of spontaneous GABA release. Several studies in the MEC found that altered the release machinery at the presynaptic terminals is accompanied by a change in the activity-dependent and evoked synaptic release (Lei et al. 2007; Wang et al. 2012). Moreover, presynaptic H_3Rs have been shown to mediate the histamine-induced reduction in activity-dependent and evoked GABA release in the striatum and ventrolateral preoptic nucleus (Ellender et al. 2011; Williams et al. 2014). Thus, it is reasonable to speculate that H_3Rs expressed at the inhibitory presynaptic terminals in the MEC might also lead to reduce the activity-dependent or evoked GABA release.

Although H_3Rs can suppress the inhibitory neurotransmission, it is noteworthy that H_3Rs also act as autoreceptors to inhibit histamine release and synthesis and restrict the release of other arousal-promoting neurotransmitters (Lin, Sergeeva, et al. 2011; Passani and Blandina 2011). The final influence of H_3Rs on brain state is governed by a balance of distinct actions across multiple brain regions. In previous behavior studies, oral administration of H_3R antagonist primarily promoted wakefulness, whereas the H_3R agonist increased cortical slow activity and slow-wave sleep (Lin et al. 1990; McLeod et al. 1998; Lin 2000). Thus, the H_3Rs exhibit constitutive activity and exert a tight control over sleep-wake cycle, which have attracted a great scientific interest for the treatment of sleep-wake disorders (Lin, Sergeeva, et al. 2011; Passani and Blandina 2011).

A Role for Histamine Innervating Superficial Layers in Modulation of Neuronal Excitability and Spatial Learning

The MEC, instead of LEC, contains spatial information-related functional cells, including grid cells, head direction cells, and border cells (Fyhn et al. 2004; Sargolini et al. 2006; Solstad et al. 2008). These results suggest that MEC circuit not only passively serves as the interface to control the flow of information into and out of the hippocampus but also is a possible neural element aiding in the integration of information about location, direction, and distance and plays an active role in spatial cognition (Fyhn et al. 2004; Steffenach et al. 2005; Witter and Moser 2006; Moser et al. 2008; Van Cauter et al. 2013). According to a dual-stage model of memory formation, encoding and consolidation of spatial memory are achieved in wakefulness and sleep, respectively, and are independently operated in the superficial and deep layers of the MEC (Chrobak and Buzsaki 1994; Buzsaki 1996; Chrobak and Buzsaki 1998; Chrobak et al. 2000; Battaglia et al. 2011; Inostroza and Born 2013). Compared with the sleep state, the principal neurons in the superficial layers of the MEC exhibit higher activity during the attentive arousal and their discharges are synchronized to the theta-coupled gamma oscillation (Chrobak and Buzsaki 1994, 1998; Isomura et al. 2006; Hahn et al. 2012; Igarashi et al. 2014). This activity pattern of the

superficial layers is correlated with that of the histaminergic system. The activity of histaminergic neurons and the central release of histamine vary in the different brain states, being lowest during sleep and awake immobility, moderate during active wakefulness, and highest during exploratory behavior (Vanni-Mercier et al. 2003; Chu et al. 2004; Takahashi et al. 2006). Moreover, histaminergic system exerts a strong control over the hippocampal theta oscillation (Masuoka et al. 2007; Hajos et al. 2008), which is known to be associated with a superficial layer-dependent memory encoding. Here, we found histamine modulates neuronal excitability and neurotransmission in a superficial layer-specific manner. Moreover, the blockade of the histamine receptors in the superficial, but not deep, layers caused impairment in rat learning phase, indicating that the endogenous histamine signaling is essential for the spatial information encoding. Despite histamine has no effects in the deep layers, dopamine, another arousal-promoting neurotransmitter (Young 2009; Qu et al. 2010), has been showed to reduce the excitability of Layer V pyramidal neurons in the EC (Rosenkranz and Johnston 2006). Thus, these results suggest that arousal-promoting systems differently regulate the neuronal activities in superficial and deep layers and thus might functionally separate the superficial and deep layers to operate memory encoding and consolidation across sleep-wakefulness cycle. Although we found negative effects of histamine in the deep layers and low expression of histamine receptors, it should be noted that deep layers of the MEC have H_1R mRNA (Lintunen et al. 1998). It is possible that these receptors might express in deep layer neuron dendrites traveling toward superficial layers. As the electrophysiological recordings were conducted at the somata, we cannot rule out the possibility that histamine affects dendritic functions and future studies are needed.

The major function of the superficial layers of the MEC may be processing incoming visuospatial information and transmitting it onto the hippocampus (Chrobak et al. 2000). The excitability of principal projection neurons in the superficial layers of the MEC exerts a tight control over the spatial learning and memory. Inhibition of neuronal excitability by the activation of $GABA_A$ or $GABA_B$ receptors dramatically impaired the rat spatial learning, whereas the increased neuronal excitability by knockdown TREK-2 channels, the final targets of the $GABA_B$ receptors, improved the learning ability (Jerusalinsky et al. 1994; Deng et al. 2009). The activity of principal neurons in the superficial layers is tightly controlled by the local GABAergic neurons (Woodhall et al. 2005; Lei et al. 2007; Buetfering et al. 2014). During a spatial memory task, high levels of endogenous histamine reduce the presynaptic GABA release and thus might disinhibit the principal neurons in the superficial layers of the MEC. This effect combined with postsynaptic excitation largely enhances the sensitivity of principal neurons to excitatory inputs and alerts the superficial layers of the MEC, thus leading to potentiation of the connection between neocortex and hippocampus and facilitation of spatial information encoding within MEC- hippocampal network (Fig. 10). Conversely in sleep, low levels of histamine and other neuromodulators disconnect the hippocampus from neocortex, leaving only internal loops operative, and enforce a bias toward memory consolidation (Tononi and Cirelli 2014). Thus, the circadian variation of the histamine and other arousal-promoting neuromodulators might induce the systematic alternation between “connected” potentiation and depression and favor

the spatial memory formation.

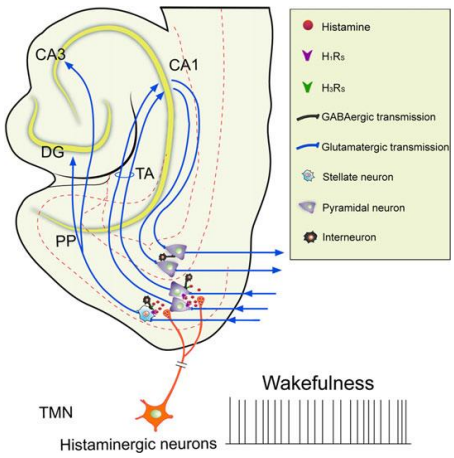

Figure 10. A diagram illustrating the MEC-hippocampal network, with reference to the action of histaminergic system and its putative physiological functions. During attentive wakefulness, high levels of histamine alert the superficial layers of the MEC via H_1Rs and H_3Rs, thus leading to potentiation of the connection between neocortex and hippocampus and spatial memory formation within MEC-hippocampal network.

The stellate and pyramidal neurons in the superficial layers of the MEC target distinct subregions of the hippocampus and serve in several features of episodic-memory processing (Kesner et al. 2000; Nakazawa et al. 2004; Nakashiba et al. 2008; Suh et al. 2011; Kitamura et al. 2014). The present study revealed no significant difference in postsynaptic effects of histamine among these principal projection neurons. As these neurons form distinct memory circuits, histaminergic indistinguishable modulation thus might contribute different aspects of the spatial learning. The present study investigated the behavior effects of histamine signaling by using a pharmacological approach, which lacks specificity. To dissect circuit-specific function of histamine, in the future study knockout of the histamine receptors in neuron type- or layer-specific manner would be much helpful.

Being enlightened by electrophysiological findings, we tested the effects of histamine signaling on spatial learning in the MEC of adult rats. Due to the influence of development, electrophysiological effects observed in rats at P14-20 might not be exactly the same as they are during adulthood. In future studies, electrophysiological recording from older rats would be much more helpful. Anyhow, the present finding is that histaminergic modulation of the superficial layers of the MEC is required for the rat spatial learning. Currently, the effect of histamine system on spatial learning has been attributed to its influence on the neuronal excitability and synaptic plasticity in prefrontal cortex and hippocampus or interaction with other neuromodulatory systems (Bacciottini et al. 2002; Luo and Leung 2010; Tsujii et al. 2010). Thus, our results provide a novel mechanism to explain at least the roles of histamine in some physiological functions such as learning and memory. Patients with schizophrenia and Alzheimer's disease, in addition to displaying neuronal pathology and atrophy of the EC (Nasrallah et al. 1997; Joyal et al. 2002; Prasad et al. 2004; Jessen et al. 2006), often exhibit abnormalities of the histaminergic system (Kim et al. 2002; Iwabuchi et al. 2005; Arrang 2007; Ligneau et al. 2007; Yanai and Tashiro 2007). Thus, abnormal modulation of MEC physiology by histamine may underlie the cognitive dysfunction in these neurological disorders.

Supplementary Material

Supplementary material can be found at: http://www.cercor.oxfordjournals.org/.

Funding

This work was funded by grants from the National Natural Science Foundation of China (No. 81071074).

Notes

We appreciate Prof. Xiaowei Chen in the Third Military Medical University, Chongqing, China, for useful advice and comments on this manuscript.

Conflict of Interest: None declared.

重要通知

2016 年国际生理学学术大会

——生命的逻辑

中国北京 2016 年 09 月 25-28 日

征文通知（再次刊登）

2012 年由中国生理学会发起，联合 9 个其他国家和地区的生理学会在苏州举办的“2012 年国际生理学学术大会”获得了空前的成功，充分展示了中国生理学会的学术水平、扩大了国际影响，为我会于 2013 年在英国伯明翰获得 2021 年国际生理学联合会 (International Union of Physiological Sciences, IUPS) 在中国召开的申办权奠定了扎实的基础。2016 年是中国生理学会成立 90 周年，学会决定召开“中国生理学会 90 周年庆典暨 2016 年国际生理学学术大会”，通过庆典活动弘扬学会传统和文化，同时为在中国召开的 2021 IUPS 大会进行准备和练兵。该学术大会定于 2016 年 09 月 25 日至 28 日在北京国家会议中心举行，详情请登录会议网站：http://www.pco-online.com/icps2016/查阅。

大会组委会已经确定特邀大会报告人 7 位，分别为中国生理学会名誉会员、美国科学院院士，UCSD 的钱煦教授，英国皇家学会院士 UCL 的 Micharl Hausser 教授，日本生学会侯任主席、Kyoto Prefectural University of Medicine 的 Yoshinori Marunaka 教授，美国科学院院士，University of Southern California 的 Larry William Swanson 教授，中国科学院院士清华大学李蓬教授、中国科学院院士，上海生命科学院张旭研究员，北京大学肖瑞平教授。

本次会议的组织形式沿用 2012 年苏州国际生理学会议的模式，即参加会议的各国家或地区学会以其学会冠名形式组织 1-3 个专题，每个专题有 4-5 个报告人，专题报告的时间是 2-2.5 小时；同时，要求其中 3 个报告人为组织该报告学会的会员，1-2 个为其他学会会员，也即每个专题报告至少要两个学会成员。报告主题由各学会根据其学会在生理学方面的研究特点确定，组织者及报告者需为相关研究领域的资深学者或有建树的青年学者。12 个国家及地区的生理学会（美国，澳大利亚，瑞士，巴西，中国台北，日本，英国，新西兰，德国，法国，斯堪的纳维亚（丹麦、芬兰、冰岛、挪威和瑞典）及心理神经免疫学会参加会议，并组织由这些学会冠名的专题报告会合计 17 个。中国生理学会提交了冠名专题报告会 20 个。合计专题报告会 37 个，涵盖了生理学各个领域。

大会报告及专题报告详细情况及日程安

排，请登录会议网页查看。

本次会议除大会报告和专题报告外，还设有青年工作者专场报告及墙报展示，具体要求详见征文范围。敬请各位会员踊跃投稿参会。

衷心感谢您对学会工作的大力支持，我们期待 9 月与各位在北京相会！

此致

敬礼！

中国生理学会理事长及大会主席王晓民

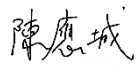

中国生理学会副理事长及大会共同主席陈应城

一、大会工作语言

英语

二、征文范围

生理科学各个领域及相关学科尚未正式发表的研究工作均在征集范围。

1、大会报告（Plenary lecture）：每个报告的时间为 40 分钟，讨论 5 分钟。以本人研究工作为主，并结合国际研究进展。报告人由大会学术委员会确定。

2、专题讨论会报告（Symposium）：每个报告的时间为 20 分钟，讨论 5 分钟。以本人研究工作为主，并结合国际研究进展。报告人由大会学术委员会确定。

3、青年工作者专场报告（Young physiologist presentation）：每个报告的时间为 8 分钟，讨论 2 分钟。报告本人最近完成且尚未正式发表的研究工作。现已开始接收投稿。青年工作者是指 1975 年 1 月 1 日之后出生的青年教师，科研人员和博士后。

4、墙报展示（Poster presentation）：墙报的内容应包括标题、作者姓名和作者单位。正文简要介绍研究目的、方法、结果（要求图、表、文并茂）和结论。现已开始接受投稿。

三、征文格式要求及截至日期

大会报告及专题讨论会报告将由大会学术委员会确定，目前主要征求青年工作者专题报告和墙报展示的稿件。**投稿的具体方法和稿件格式请参看会议网页中有关投稿事宜**。投稿截止日期：**2016 年 6 月 15 日**。

四、会议注册，交费和住宿预订

1、旅费和住宿费自理。

2、会议将收取注册费（包括会议论文集出版费用和中餐费等）。

3、会议采用网上注册、交费和住宿预订，具体事宜请参看会议网页。

分类	2015 年 12 月 01 日至 2016 年 07 月 31 日	2016 年 08 月 01 日至 2016 年 08 月 31 日	2016 年 09 月 01 日至 2016 年 09 月 28 日
国内正式代表	人民币 1800 元/人	人民币 2200 元/人	人民币 2500 元/人
国内学生代表	人民币 900 元/人	人民币 1100 元/人	人民币 1300 元/人

注：学生注册时需要出示学生证，博士后须按正式代表注册。

五、会议网址

http://www.pco-online.com/icps2016/。关于大会准备工作的进程，请随时登陆查看网页的更新。

马兰教授荣获第七届“全国优秀科技工作者”称号

马兰教授，1958 年出生，1982 年获沈阳药学院学士学位，1984 年获中国医科大学硕士学位，1990 年获美国北卡罗莱纳大学博士学位，1991-1995 年分别在美国北卡罗莱纳大学和拜耳公司制药部研究中心从事博士后研究。1995 年回国任上海医科大学（现复旦大学上海医学院）教授至今。

马兰教授现任复旦大学脑科学研究院院长、药理研究中心主任。教育部“长江学者奖励计划”特聘教授、国家杰出青年科学基金获得者；兼任复旦大学学术委员会委员、中国生理学会副理事长、学术工作委员会主任委员、中国神经科学学会常务理事、Sci Rep、Neurosci Bull、Front Neuroendocrine Sci 等杂志编委。

马兰教授的主要研究方向为精神药物成瘾的分子机理，为“阿片类物质精神依赖的神经生物学机制”（2009-2013）、“精神活性物质成瘾记忆的形成和消除”（2015-2019）973 项目首席科学家和“精神药物成瘾与记忆的机制”（2009-2011，2012-2014，2015-2017）基金委创新研究群体带头人。近年来的研究工作阐述了 GRK 和 PKC 等蛋白激酶对阿片受体介导的神经信号转导的负调控及其分子机制，揭示了阿片类药物对神经突触可塑性的影响及学习记忆在阿片类耐受和依赖形成中的关键作用，发现了阿片类药物通过表观遗传学修饰机制调控脑基因表达的新途径和 β-arrestin 作为核信使的新功能，为开发创新镇痛药物和戒毒药提出了新思路。已在 Cell、PNAS、J Cell Biol 等刊物发表 SCI 论文 100 余篇，其中关于蛋白激酶的工作获得国家自然科学二等奖；关于药物调控靶基因转录的表观遗传学新机制的研究入选 2005 年度中国医药科技十大新闻和 2005 年度上海十大科技进展；关于 GRK5 在神经系统中的功能的研究成果入选两院院士评选“2011 年中国十大科技进展新闻”和 2011 年度上海十大科技进展。上述研究成果获得国家自然科学二等奖（2002、2006）2 项、以及省部级科技进步一等奖 6 项，并获得何梁何利科学与技术奖、香港求是杰出青年学者奖等荣誉。

经中国生理学会推荐，全国优秀科技工作者评审委员会评审、中国科协全国委员会常务委员会批准，马兰教授于 2016 年荣获第七届“全国优秀科技工作者”称号。

王世强教授荣获第七届“全国优秀科技工作者”称号

王世强教授，1990 年毕业于北京大学生物学系，留校任教。1998 年在北京大学获生理学博士学位。任教以来，一直以饱满的热情勤奋从事教学和科研工作，坚持教学、科研并重，科研与科普相结合。

一、潜心教书、精心育人

知识与思维的有机结合是创新的基础。王世强教授承担生理课教学，提倡通过思考融会贯通，防止死记硬背，围绕培养创新能力精心设计每个教学环节。通过重要科学史实和科学争论、经典实验设计、生理原理的解析计算

等，培养逻辑思维、创新意识和运用知识解决问题的能力。

生物学是实验学科。王世强教授强调实验课与理论课密切配合产生协同效果。将生理实验内容赋以研究性和自主性，强调对不预期实验事实的捕获和深入分析，引导学生通过实验事实重新发现理论知识，培养学生发现与创新的意识。

学生在课堂学习、实验、文献阅读中会产生不同问题和看法。王世强教授籍此定期开展小班讨论，结合实验现象和前沿问题引导学生主动获取知识，培养创新思维。

为配合以创新能力为核心的教学改革，王世强教授与复旦大学梅岩艾教授、南京大学王建军教授共同主编了综合大学适用的《生理学原理》（高等教育出版社 2011），在生理机制分析、结构与功能并举、生理功能的进化和适应、科学发现的典型案例等方面具有特色，强化创新思维的培养。

以上教学改革受到学生普遍欢迎。所讲授的生理学及实验是北大生命科学学院学生喜爱的课程之一。1991 年以来 6 次荣获北京大学教学奖，2013 年获北京市优秀教师称号。

二、把握前沿、锐意创新

王世强教授长期从事钙稳态和钙信号转导的前沿研究，1994 年起在国内最早用激光共聚焦显微术研究细胞钙信号，发现冬眠动物能防止细胞钙超载，机制是钙内流下调和肌质网钙转运上调。由此提出并找到改善非冬眠动物心肌钙稳态和耐寒性的途径，不仅揭示了冬眠动物耐寒适应的关键机制，更对低温医学有重要意义。这些完全在国内完成的工作获 1997 中国生理学会张锡均一等奖、2001 美国生理学会 Scholander 比较生理奖（每年只评一人），英国《实验生物学报》作专题报道。

钙信号转导是兴奋收缩耦联的关键。为了探明其分子过程，王世强教授与程和平院士克服系列技术难关，首次用光学方法记录单通道钙信号，命名为 Ca sparklet。基于此设计了松箝技术，首次测定钙通道触发肌质网钙释放通道 RyR 的随机动力学和分子效率，发现 RyR 电流量子化现象和特殊的高斯动力学，提出并证明 RyR 热力学不可逆变构学说。这些工作发表于《自然》、《美国科学院报》等，将细胞钙信号转导研究推进到单分子水平，结束了学界十多年关于钙火花本质的争论。获美国生理学会细胞分子生理学奖、美国心脏学会 Katz 基础科学研究奖、国际心脏研究会理查德·冰奖。

交感神经是心搏的主要调控机制，RyR 是控制心脏收缩力的关键离子通道，但因其位于细胞内肌质网不能直接记录，其是否受到交感受体调控长期争议不休。王世强实验室通过独到设计，首次确证肾上腺素受体通过 PKA 调控 RyR 钙释放敏感性，发表于《美国科学院报》等刊。这不仅解决了该领域十几年的学术争论，也培养了人才。他指导的博士生周鹏因此获得 2006 国际药理联合会青年研究者奖，并被著名神经科学家、诺贝尔奖获得者 Tom Südhof 院士直接录取为博士后。

王世强教授在科研选题方面注重将基础研究与人类疾病问题紧密结合。近十年来重点研究心力衰竭的病理分子机制，不断取得突破进展，发现心衰细胞钙通道与肌质网 RyR 耦联效率衰退，关键原因是 miR-24 下调 JP2 使钙通道与 RyR 脱耦联；抑制 miR-24 则阻止心衰病理发展。这些成果在《PLoS 生物学》、美国《循环研究》等高影响期刊发表，获卫生部中国有突出影响心血管论文奖。《自然·评论·药物发现》、《循环研究》、欧洲《心血管研究》分别发表亮点述评，高度评价这些发现“揭开心脏疾病分子机制的面纱”，为心衰诊断和防治开辟了新思路。这也是王世强任首席科学家的 973 项目的重要成果。

以上研究在心脏钙稳态和钙信号领域形成特色并产生重要学术影响。国际同行主动联

系请王世强教授担任第 17 届国际钙结合蛋白大会（2011）主席，是该系列国际会议首次由发展中国家主办。

三、投身科普、关注少年

青少年时期是启迪科学兴趣、培养科学意识的黄金时期。王世强教授在繁重的教学科研同时还积极投入科普活动。每年暑期给中学生举行科普讲座，并业余撰写科普文章，受到广大青少年喜爱，获得 2013 年北京市优秀科普作品奖。

经中国生理学会推荐，全国优秀科技工作者评审委员会评审、中国科协全国委员会常务委员会批准，王世强教授于 2016 年荣获第七届“全国优秀科技工作者”称号。

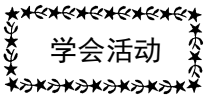

中国生理学会“第十一届全国生理学教学研讨会”成功召开

2016 年 7 月 2 日-3 日，由中国生理学会主办，大连医科大学承办的中国生理学会“第十一届全国生理学教学研讨会”在辽宁省大连市举行。本次会议共收到论文摘要 121 篇（刊登在《生理通讯》第 35 卷增刊 I 上，2016），来自全国 88 所院校的 220 余位生理学工作者参加了会议。中国生理学会副理事长王韵教授、管又飞教授和罗自强教授参加了此次会议。

大会开幕式由中国生理学会教育工作委员会副主任委员、中山大学中山医学院王庭槐教授主持。中国生理学会副理事长、大连医科大学副校长管又飞教授代表大连医科大学向与会的兄弟院校的领导和教师表示欢迎，并对各高校一直以来的大力支持和帮助表示感谢，希望通过两天的讨论交流，能够有效带动生理学教学水平的整体提升。中国生理学会副理事长兼秘书长、北京大学医学院王韵教授致辞，向多年来致力于生理学教学的各位专家和学者表示亲切的问候。中国生理学会副理事长、教育工作委员会主任委员、本次大会主席、中南大学罗自强教授致辞，并指出本届教学研讨会是继 2012 年在南昌举行第十届研讨会后的再次相聚，是学会主办全国教学研讨会以来参加单位数及参会人数最多的一次盛会。希望大家互相学习、增进友谊，共同促进生理学教学工作的发展。

开幕式后是 7 个大会特邀报告。王庭槐教授首先对生理学实验教学改革三十年进行了回顾与展望，随后王韵教授介绍了学科与器官系统整合体系下的生理学教学，管又飞教授做了题为“培养创新和应用兼顾型医学人才的教学改革实践”的报告。中国生理学会常务理事、南京大学生命科学学院王建军教授向参会学者介绍了生理学名词审定的工作。罗自强教授做了题为“以胜任力为导向开展生理学教学综合改革的思考与实践”的报告，中南大学湘雅医学院秦晓群教授介绍了基础医学实验设计大赛如何助推研究型学习，南京医科大学高兴亚教授阐述了对医学教育信息化的发展与展望。

本届教学研讨会对生理学教学领域进行回顾和展望，结合生理学教学改革、学科建设、教学方法、师资培养、双语教学、研究生教育、课程建设、新媒体技术的应用等 13 个领域设立了 2 个分会场共进行了 39 场高端教学会议报告，为与会师生带来了一场教学盛宴，搭建了高校间面对面深入交流的平台。专家们从多角度阐述生理学教学的改革、创新，并从当前生理学发展的趋势，对当今生理学教学发展所

面临的挑战进行了分析和讨论。会议期间许多年轻教师在报告过程中对生理学教学方法、教学改革、实验课内容设置以及网络教学等领域提出了自己的看法、思路与建议，与在场各专家学者进行了充分的交流。参会者对报告内容进行提问，现场气氛热烈。

3 日下午，与会者在朱亮副院长的带领下参观了大连医科大学基础医学院生理学教研室和国家级实验示范中心，参会教师在教学工作、教学课程改革、大学生科研等方面与在校教师进行了探讨和交流，为学校教学和科研的发展提出了建设性意见。

本次生理学教学研讨会不仅达到了教学交流的目的，与会专家也对生理学教学发展的意义和重要性达成了广泛共识。专家们对生理学教学改革的具体实践进行了深入探讨，并且为学校生理学学科发展提供了新思路。

（大连医科大学供稿）

2016 中国生理学会新型生理学实验技术平台培训班圆满结束

刘　璐

（中国生理学会办公室　北京　100710）

由中国生理学会主办、贵州医科大学承办、成都泰盟软件有限公司协办的“中国生理学会新型生理学实验技术平台培训班”于 2016 年 7 月 25-31 日在贵州贵阳如期举办。

来自21个省46个单位的100名生理科学工作者参加了学习。

贵州医科大学基础医学院常务副院长杨明教授及基础医学院基础医学实验教学中心多媒体机能学实验室主任李玲教授等领导对此次学习班高度重视，出席了学习班开幕式并讲话。中国生理学会副理事长、中南大学湘雅医学院罗自强教授代表中国生理学会发言，强调了生理学教学的重要性，同时感谢承办方和协办方对中国生理学会举办这次培训班的支持，并欢迎来自全国各个学校参与培训班学习和交流的生理学工作者们。

随后山东大学医学院刘传勇教授、中南大学湘雅医学院秦晓群教授、罗自强教授均分别进行了精彩报告。刘传勇教授首先做了题为“推进实验教学改革，培养优秀医学人才”的报告，报告中向大家讲授了“新世纪医学实验教学三端改革”、“山东大学医学基础实验中心建设”以及“虚拟仿真实验教学中心建设的探索与实践”三个部分内容，分析了目前高校虚拟实验教学资源未得到充分利用所存在的问题，并对机能学虚拟实验教学的未来进行了展望。秦晓群教授所讲授的题目为“基础医学实验设计大赛助推研究型学习”，并向大家介绍了“研究型学习”及历届基础医学实验设计大赛的举办情况和效果。罗自强教授为学员们讲授了题为“翻转课堂的实施与思考”的精彩报告，重点介绍了翻转课堂相关概念及应用体会，并对如何提升课堂教学质量进行了探讨与思考。随后成都泰盟软件有限公司的黄武董事长做了题为“基于信息化的下一代生物信号采集与处理系统介绍”以及“最新VR技术在医学虚拟仿真实验教学中心的应用”的报告，徐国标副总经理进行了“药理和行为学研究设备应用技术探讨”的报告。现场各学员认真聆听、学习并交流讲授内容，踊跃提问，并进行热烈讨论，学员们纷纷表示获益匪浅。

在随后几天的学习中，贵州医科大学和泰盟公司在贵州医科大学基础医学院实验教学中心医学技能实验室共同开展了演示实验及教学实验，实验内容涉及生理无线遥测实验技术，血管环张力试验，无创血压测定等多项演示实验，并将生物分子实验与VR技术相结合，使学员进行亲身体验。教学内容包含神经干动作电位引导、呼吸运动调节等多项内容。贵州医科大学的各位授课老师十分负责，为培训班相关的实验教学进行了充分的准备，学员们认真学习观摩，对教学和演示实验的关键内容进行拍摄和记录，并积极参加实践操作，互相交流和讨论相关经验，受益良多。其间，学会还组织学员们一同参观了贵州医科大学生命科学馆，观看了生物学、人体寄生虫学、人体组织与胚胎学、人体解剖学和法医学等学科的大量珍贵标本。

在实验教学期间，学会与泰盟公司共同开展了“机能实验技能比赛”，比赛共进行了10组，学员们自行组队，通过在BL-420N操作系统上模拟，对相关实验内容进行理论考核和实践考核，最终对完成效果最佳的团队进行表彰和颁奖。此次技能比赛为培训班首次开展，学员们均积极报名参与，达到优良效果。通过参加竞赛，各学员不仅进一步学习了比赛内容中加强重视的理论知识和实践知识，更增进了团队间的合作能力，并同时提供了大家相互间交流的机会。

本次培训班的开展获得了良好效果和成功经验，学员们感到获益匪浅，并对学习班的整体安排感到满意。学会在来年会继续举办继续教育培训班，欢迎生理界同仁踊跃参加与交流。

大连医科大学肾脏病中心成立大会、医学科学研究院第二届学术年会暨中国生理学会肾脏生理专业委员会第三届学术年会圆满召开

栾志林　陈丽红

（大连医科大学医学科学研究院　辽宁大连　116044）

7 月 26 日-28 日，大连医科大学肾脏病中心成立大会、医学科学研究院第二届学术年会暨中国生理学会肾脏生理专业委员会第三届学术年会在我校图书馆学术报告厅举行。中国工程院院士陈香美教授、中国工程院院士宁光教授，学校党委书记周万春、党委副书记靳媛、副校长邹存慧、副校长佟春光，党委常委、附属第二医院院长赵作伟，校长助理田晓峰出席成立大会。香港中文大学李嘉诚健康医学研究所副所长蓝辉耀教授、英国 Leicester 大学医学院副院长 Kevin Harris 教授等一行 5 人、俄亥俄州立大学胸外科讲席教授麻建杰教授、深圳大学千人计划专家阮雄中教授等多位国内外从事肾脏生理、病理生理和转化医学研究的基础和临床的著名专家应邀出席开幕式并作学术报告。中国生理学会肾脏生理专业委员会全体理事，来自医学科学研究院、基础医学院、第一附属医院、第二附属医院、大连市中心医院、解放军 210 医院、江苏苏北人民医院的领导和肾脏病专家，学校职能部门负责人、学校师生代表和来自全国各地的研究人员共 400 余人参加了中心成立仪式及为期两天的学术会议。

26 日下午，副校长管又飞主持开幕式并介绍了肾脏病中心成立的背景。党委副书记靳媛宣读了《关于成立大连医科大学肾脏病中心的的决定》。

党委书记周万春和陈香美院士共同为大连医科大学肾脏病中心揭牌。

周万春书记在成立大会上致辞。他代表学校党委以及全体师生员工向大连医科大学肾脏病中心的成立表示衷心的祝贺，并对医学科学研究院成立一年来取得的丰硕科研教学成果表示肯定和赞扬。周书记还向不辞辛苦，远道而来的国内外知名专家、领导和嘉宾的到来表示诚挚的欢迎和感谢。周书记指出，大连医科大学肾脏病中心将不仅是国内外肾脏研究学术交流和协作的平台，更将大力促进转化医学研究，加强肾脏生理与心血管、代谢及肿瘤等疾病的交叉和融合，促进基础、临床和相关

领域间的跨学科发展。此次大会也将加强国内外肾脏学科基础和临床研究工作者的沟通与交流，提升大连及周边地区肾脏病学在国内外同行的影响力及学术地位。

随后，陈香美院士作了题为《我国肾脏疾病防治的现状、挑战和对策》的主题报告。陈香美院士着重介绍了我国肾病防治的严峻形势、研究现状及应对策略，并希望大连医科大学肾脏病中心能在基础和临床整合、转化及精准医学研究方面做出重要贡献。

为期两天的学术会议聚焦肾脏科学学科前沿和热点，共举行了 21 场高端学术报告，来自国内外的著名专家们从多个角度介绍了近年来肾脏病领域在病因和机制研究及诊疗方面取得的新进展，并在学科建设、教学和实验技术方面进行了广泛的交流，学术活动氛围浓厚、热烈。

会议期间还举行了大连医科大学免疫和代谢性肾脏病研究所成立仪式。医学科学研究院特聘教授、附属第二医院肾内科主任郑丰教授主持仪式并介绍了研究所的成立背景。

副校长管又飞教授致辞。他总结了医学科学研究院在过去一年中所取得的进步，并强调免疫及代谢异常在肾脏病发生发展中的重要作用，以及成立免疫和代谢性肾脏病研究所的必要性。他希望研究所能够凝练学科特色、引进培养人才、建设高端平台、推进转化研究，为肾病防治做出贡献。

中国工程院院士宁光教授、副校长管又飞教授、附属第二医院院长赵作伟教授、英国莱斯特大学免疫、感染和炎症性疾病系 Peter Andrew 教授等共同为研究所揭牌。

揭牌仪式后，赵作伟院长在致辞中表示，肾脏作为在维持生命健康中发挥着重要功能，免疫和代谢性肾脏病研究所的成立必将不断地在学术研究以及成果转化上实现良好的发展，成为大连医科大学科技创新、人才培养以及社会服务的重要基地。

中国工程院院士宁光教授作了题为《中国糖尿病的现状、挑战及精准治疗》的主题报告。宁光院士就目前我国糖尿病防治面临的巨大挑战、目标和任务做了深入的讲解。他希望全国糖尿病领域的专家学者和临床工作者携起手来，开展协同创新研究，共同为我国糖尿病患者提供最好的医疗服务。

为鼓励肾脏病领域青年科研人才的学术成长，本次会议还特设了青年学者报告专场，开展了墙报学术交流，并对优秀墙报进行了表彰。

最后，上海复旦大学、中国生理学会肾脏生理专业委员会秘书长陆利民教授致闭幕辞，他代表中国生理学会对肾脏病中心的成立表示衷心祝贺。他指出，中国肾脏并防治工作仍然面临重大挑战，希望大连医科大学肾脏病中心在未来能得到快速发展，能够成为国内肾脏病基础和临床研究的重要基地。他表示，中国生理学会肾脏生理专业委员会成立近 10 年，聚集了一大批国内肾脏领域基础和临床的精英人才，始终致力于基础和临床的结合，着力打造国际合作交流的平台，并将培养肾脏领域的青年人才列为重要目标。

会议期间，英国莱切斯特大学代表团与学校国际交流合作处、教务处、研究生院、国际教育学院的领导商谈了两校在医教研领域的合作，在建立两校友好合作关系、开展本科生的长短期交流、研究生联合培养、开展肾脏病专业博士 2+1 项目达成了共识。

2016 年中国生理学会心血管生理学术研讨会会议纪要

张鸣号
（宁夏医科大学　宁夏银川　750004）

2016 年中国生理学会心血管生理学术研讨会于 2016 年 8 月 12-14 日在塞上江南宁夏回族自治区首府银川市胜利召开。本届会议由中国生理学会循环生理专业委员会主办，宁夏医科大学承办。共有来自全国 35 家医学院校和科研院所的 120 位专家学者和研究生参加了本次学术研讨会。

中国生理学会循环生理专业委员会在 2016 年 8 月 12 日晚召开了中国生理学会循环生理专业委员会全体会议。宁夏医科大学张鸣号副教授代表组委会向专委会汇报了大会筹备情况，专业委员会主任委员、大会主席曾晓荣教授对宁夏医科大学的会议组织工作给予了充分肯定和感谢。经专业委员会全体委员讨论，决定下一届研讨会由中山大学中山医学院承办。

大会开幕式由中山大学王庭槐教授主持，宁夏医科大学牛阳副校长致欢迎词，国家基金委医学部孙瑞娟副主任、宁夏回族自治区科协陈国顺副主席、中国生理学会循环生理专业委员会主任委员、大会主席曾晓荣教授出席了开模式，并分别向大会致辞。

2016 年 8 月 13 日至 14 日，首都医科大学附属北京安贞医院杜杰教授、北京大学医学部唐朝枢教授、西南医科大学曾晓荣教授等分别为大会作了题为“炎症与心血管损伤”、“心血管生理学研究热点问题分析”及“离子通道与心脏疾病”的精彩特邀报告。中国医学科学院基础医学研究所曹济民教授、首都医科大学刘慧荣教授、第二军医大学王伟忠教授、同济大学林丽教授、中国科学院上海生命科学研究所/上海交通大学医学院健康科学研究所杨黄恬教授等为大会作了主题报告。同时，经过大会学术委员会的评选，来自全国的 11 位青年

学者入选了青年优秀论文报告专场。最终，来自北京大学医学部的王美丽获得了一等奖，首都医科大学基础医学院的张苏丽和北京大学医学部生理学系俞冰获得二等奖，四川大学华西医院心血管疾病研究室李君丽、中国医学科学院基础医学研究所蔺彩霞和西南医科大学心血管医学研究所李光获得了三等奖。

大会闭幕式由孔炜教授主持，曾晓荣教授进行大会总结发言，曹济民教授宣读优秀青年论文获奖者名单，唐朝枢教授和袁文俊教授等为获奖的青年学者进行了颁奖。王庭槐教授代表中山大学作为下一届大会承办单位代表进行了表态发言。最后，孔炜教授宣布“2016年中国生理学会心血管生理学术研讨会”胜利闭幕。

《生理通讯》
（双月刊）
2016 年第 35 卷第 4 期
（内部发行）
8 月 31 日出版

主　　办：中国生理学会
编辑、出版：《生理通讯》编辑部
（北京东四西大街 42 号中国生理学会　邮编：100710）
印刷、装订：廊坊市光达胶印厂
会 员 赠 阅

中国生理学会　电话：（010）65278802　（010）85158602　传真：（010）65278802　准印证号：Z1525—981277
网址：http://www.caps-china.org/　**电子信箱**：xiaoling3535@126.com　zgslxh@126.com
责任编辑　肖　玲　刘　璐

北京新航兴业科贸有限公司

YP100 型压力换能器（免定标），经过多年的研究、改进，为了更好地适应生理、药理、机能实验教学的需要，对换能器做出了三大突破性的改进。
一、免定标：换能器在生产过程中做到了输出一致性，每支换能器的灵敏度都小于 1%的误差，在教学过程中可直接把换能器的输出 mv 输入到采集系统中，不需定标，另外每支换能器之间可以互换。
二、过载大：换能器的测量范围-50~300mmHg，精度小于 0.5%，为了保证使用安全，换能器在设计中加了防过载装置，使换能器的过载可达 2000mmHg 以上，这样就防止了学生加液体时操作失误造成的换能器损坏。
三、免清洗：换能器在实验使用中有回血现象，使用完后必须对换能器进行清洗，如果清洗不当，会造成换能器的损坏，为了避免这种情况的发生，我们设计了隔离罩，让换能器与液体隔开，使用后只清洗换能器的罩子，无需清洗换能器。改进后的换能器，它的使用寿命大大增加，该换能器适用于成仪，泰盟，美易，澳大利亚，BIOPAC 的采集系统。
YP200 型压力换能器，（免定标）
JZ100 型张力换能器（免定标）是公司最近研制的它可以调零、调增益，它可以与成仪、泰盟、的采集系统配套，（成仪 30g/100mv、泰盟 50g/50mv），为了使用安全，换能器的应变梁上下加了保护装置。
XH200 型大鼠无创血压测量仪
该仪器自动加压，可同时测量 1-6 只大鼠的尾压，可与成仪、泰盟、美易的采集系统配套使用。
XH1000 型等长张力换能器 测量范围：0-10g 0-30g 0-50g 0-100g 0-300g 0-500g
XH200 型等长收缩换能器 测量范围：0-3g 0-5g 0-10g 0-20g 0-30g 0-50g
DZ100 型等张力换能器（长度变化） 测量范围：±20 mm
XH1000 型痛觉换能器（用于足底刺痛） 测量范围：0-100g 0-200g 0-300g 0-500g 0-1000g
HX100 型呼吸换能器（人体胸带式）
HX101 型呼吸换能器（动物捆绑式）
HX200 型呼吸流量换能器（插管式）
HX300 型呼吸换能器（单咀式 连接丫字插管式或动物鼻孔）
HX400 型呼吸功能换能器（人体呼吸波、肺活量等测量用）
HX500 型插管式呼吸波换能器（用于兔子、大鼠、小鼠插气管或插鼻孔）
XH100 型小鼠呼吸实验盒（用于咳嗽药物实验）
WS100 型胃肠运动换能器（用于测量胃肠蠕动）
YL200 型力换能器（用于测量动物某个部位的折断力 最大拉力为 2000g）
CW100 型温度换能器（用于测量动物的肛温 探头为 Ø2×10mm）
CW200 型温度显示测量仪
CW300 型肛温换能器（用于测量动物的肛温，探头为 Ø3×50mm）
CW400 型片式体温换能器（用于测量动物表面体温）
XJ100 型心音换能器（用于人和动物的心音测量）
XJ200 型两用听诊器（用于教学实验 听声音与记录同步）
MP100 型脉搏换能器（用于测量人的指脉）
MP200 型鼠尾脉搏换能器（用于测量大鼠或小鼠的尾脉）
MP300 型腕部脉搏换能器（用于测量人的手腕部位的脉搏）
人体血压测量教学套件（用于无创血压测量 由血压表、压力换能器、电子听诊器组成）
其它附件：一维不锈钢微调器、二维微调器、三维微调器、神经屏蔽盒、进口三通、铂金电极、记滴换能器、电极万向夹
以上产品都能与成都仪器厂、南京美易、成都泰盟、澳大利亚 BLOPAC 等国内外采集系统配套使用。

公司名称：北京新航兴业科贸有限公司
地址：北京市朝阳北路 199 号摩码大厦 1018 室
电话：（010）85985769 （010）85987769（传真）
邮编：100026
网址：www.xinhangxingye.com
邮箱：http://mail.yan85985769@sina.com 13701369580@163.com